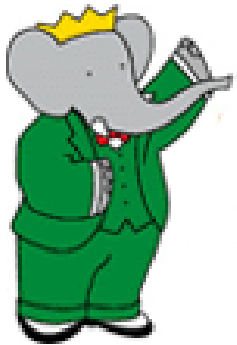


# Precise Measurement of the $e^+e^- \rightarrow \pi^+\pi^-(\gamma)$ Cross Section with BaBar and the Muon $g-2$

Michel Davier (LAL – Orsay, BaBar Collaboration)



- the muon magnetic anomaly
- $e^+e^-$  and (revisited)  $\tau$  spectral functions
- the BaBar ISR (Initial State Radiation) analysis
- test of the method:  $e^+e^- \rightarrow \mu^+\mu^-(\gamma)$
- results on  $e^+e^- \rightarrow \pi^+\pi^-(\gamma)$
- combination of all  $ee$  data
- discussion and perspectives



# Lepton Magnetic Anomaly: from Dirac to QED

$$\vec{\mu} = g \frac{e}{2m} \vec{s},$$

$$a = (g - 2)/2$$

Dirac (1928)  $g_e=2$   $a_e=0$

anomaly discovered:

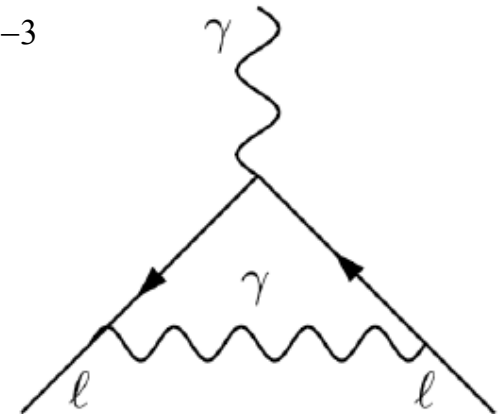
Kusch-Foley (1948)  $a_e = (1.19 \pm 0.05) 10^{-3}$

and explained by  $O(\alpha)$  QED contribution:

Schwinger (1948)  $a_e = \alpha/2\pi = 1.16 10^{-3}$

first triumph of QED

$\Rightarrow a_e$  sensitive to quantum fluctuations of fields



# More Quantum Fluctuations

$$a = a^{\text{QED}} + a^{\text{had}} + a^{\text{weak}} + ? a^{\text{new physics}} ?$$

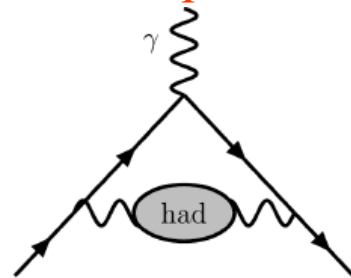
typical contributions:

**QED** up to  $O(\alpha^4)$ ,  $\alpha^5$  in progress (Kinoshita et al.)

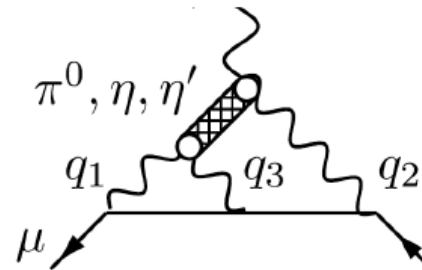


**Hadrons**

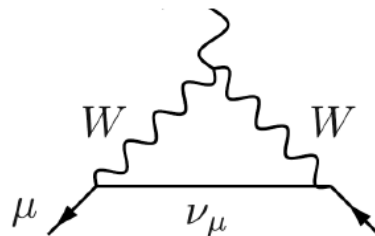
**vacuum polarization**



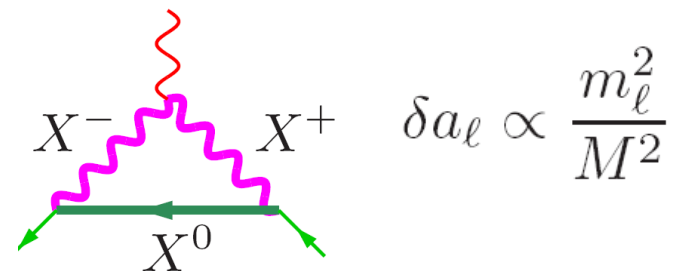
**light-by-light** (models)



**Electroweak**



new physics at high mass scale



$$\delta a_\ell \propto \frac{m_\ell^2}{M^2}$$

$\Rightarrow a_\mu$  much more sensitive to high scales

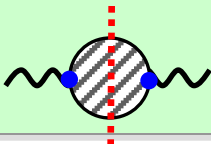
# Hadronic Vacuum Polarization and Muon $(g-2)_\mu$

Dominant uncertainty from lowest-order HVP piece

Cannot be calculated from QCD (low mass scale), but one can use experimental data on  $e^+e^- \rightarrow \text{hadrons}$  cross section

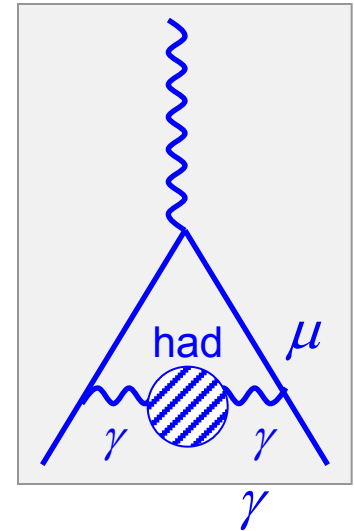
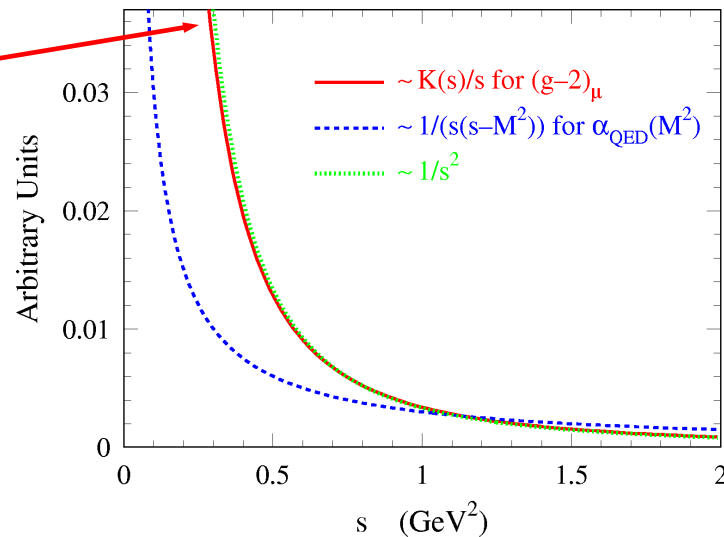
$$\text{Born: } \sigma^{(0)}(s) = \sigma(s)(\alpha / \alpha(s))^2$$

$$12\pi \text{Im}\Pi_\gamma(s) = \frac{\sigma^0[e^+e^- \rightarrow \text{hadrons}(\gamma)]}{\sigma_{pt}} \equiv R(s)$$

$$\text{Im}[\text{diagram}] \propto |\text{diagram hadrons}|^2$$


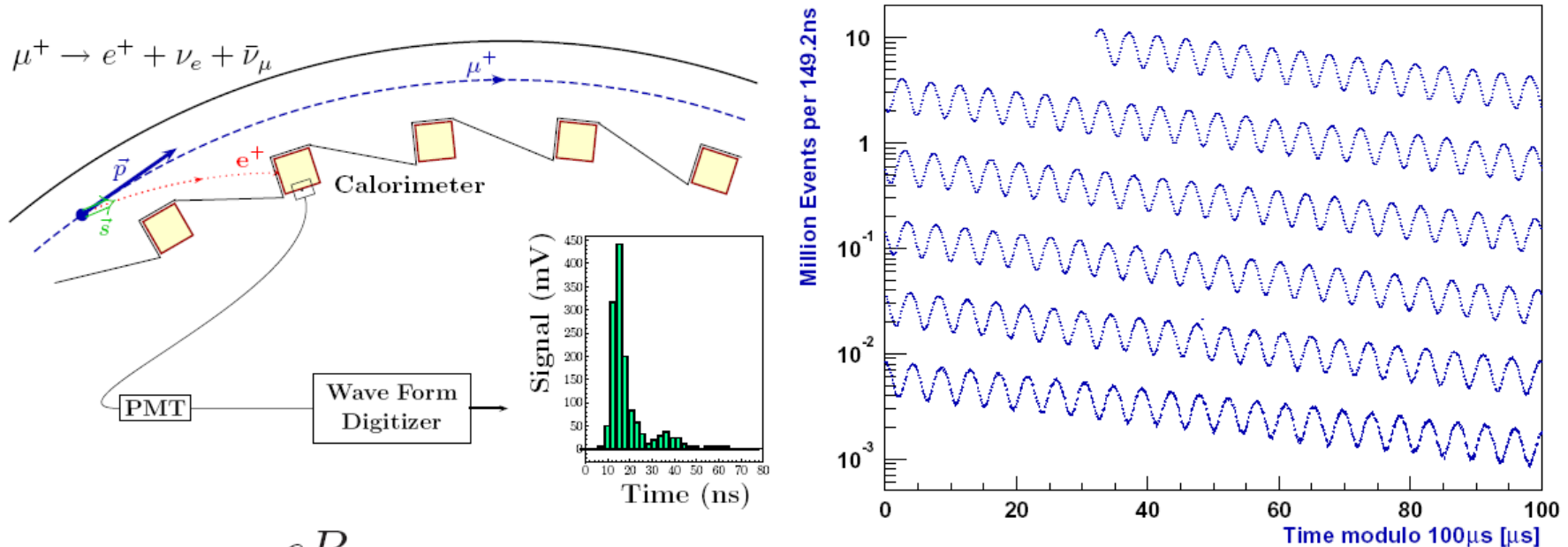
$$a_\mu^{\text{had}} = \frac{\alpha^2}{3\pi^2} \int_{4m_\pi^2}^{\infty} ds \frac{K(s)}{s} R(s)$$

Dispersion relation



# The E-821 Direct $a_\mu$ Measurement at BNL

Storage ring technique pioneered at CERN (Farley-Picasso...)



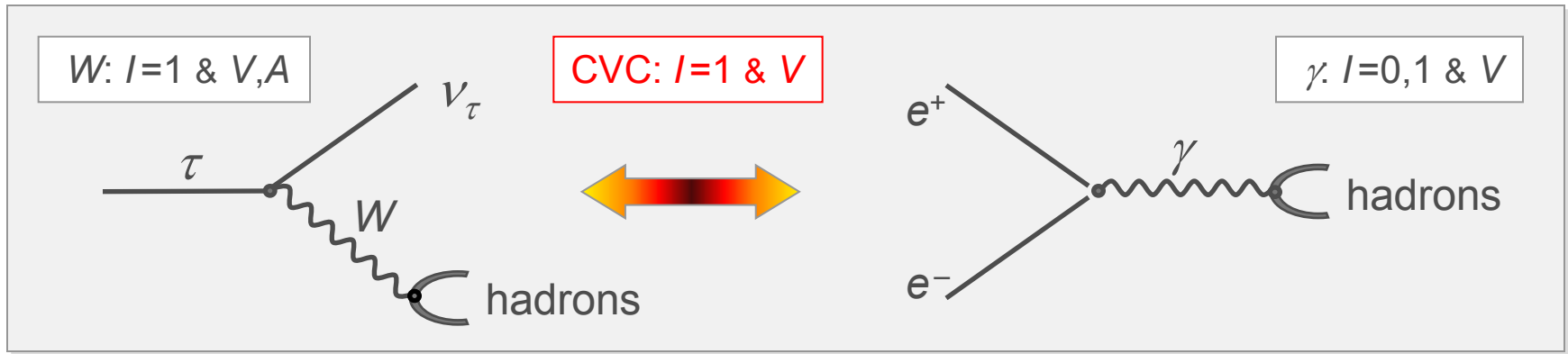
$$\omega_a = a_\mu \frac{eB}{m_\mu}$$

$a_\mu$  obtained from a ratio of frequencies  
 result updated with new value for  $\mu_\mu/\mu_p$  ( $+0.9 \cdot 10^{-10}$ )  
 (see next review in RPP2009 (Hoecker-Marciano))

$$\omega_{\text{precession}} - \omega_{\text{rotation}}$$

$$a_\mu^{\text{exp}} = (11\,659\,208.9 \pm 5.4 \pm 3.3) \cdot 10^{-10} \\ (\pm 6.3) \quad (0.54 \text{ ppm})$$

# The Role of $\tau$ Data through CVC – SU(2)



Hadronic physics factorizes (spectral Functions)

$$\sigma^{(I=1)}[e^+e^- \rightarrow \pi^+\pi^-] = \frac{4\pi\alpha^2}{s} \nu[\tau^- \rightarrow \pi^-\pi^0\nu_\tau]$$

$$\nu[\tau^- \rightarrow \pi^-\pi^0\nu_\tau] \propto \underbrace{\frac{\text{BR}[\tau^- \rightarrow \pi^-\pi^0\nu_\tau]}{\text{BR}[\tau^- \rightarrow e^-\bar{\nu}_e\nu_\tau]}}_{\text{branching fractions}} \underbrace{\frac{1}{N_{\pi\pi^0}} \frac{dN_{\pi\pi^0}}{ds}}_{\text{mass spectrum}} \underbrace{\frac{m_\tau^2}{(1-s/m_\tau^2)^2 (1+s/m_\tau^2)}}_{\text{kinematic factor (PS)}}$$

# SU(2) Breaking

Corrections for SU(2) breaking applied to  $\tau$  data for dominant  $\pi^-\pi^+$  contrib.:

## ■ Electroweak radiative corrections:

- ▶ dominant contribution from short distance correction  $S_{EW}$
- ▶ subleading corrections (small)
- ▶ long distance radiative correction  $G_{EM}(s)$

Marciano-Sirlin' 88

Braaten-Li' 90

Cirigliano-Ecker-Neufeld' 02  
Lopez Castro et al.' 06

## ■ Charged/neutral mass splitting:

- ▶  $m_{\pi^-} \neq m_{\pi^0}$  leads to phase space (cross sec.) and width (FF) corrections
- ▶  $\rho$ - $\omega$  mixing (EM  $\omega \rightarrow \pi^-\pi^+$  decay) corrected using FF model
- ▶  $m_{\rho^-} \neq m_{\rho^0}$  \*\*\* and  $\Gamma_{\rho^-} \neq \Gamma_{\rho^0}$  \*\*\*

Alemany-Davier-Höcker' 97, Czyż-Kühn' 01

Flores-Baez-Lopez Castro' 08  
Davier et al.' 09

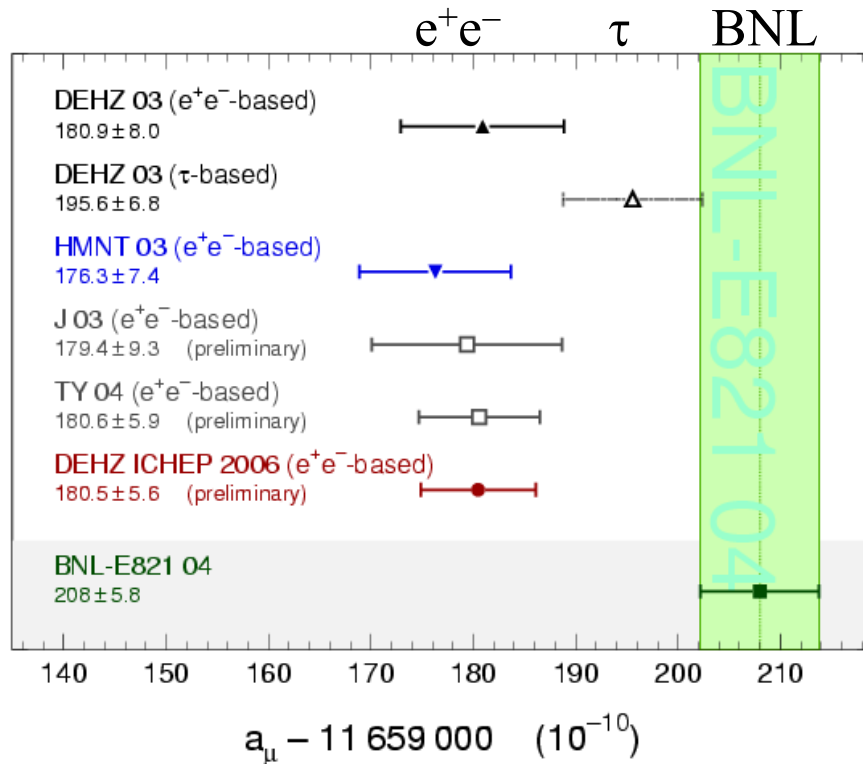
## ■ Electromagnetic decays: $\rho \rightarrow \pi\pi\gamma$ \*\*\*, $\rho \rightarrow \pi\gamma$ , $\rho \rightarrow \eta\gamma$ , $\rho \rightarrow l^+l^-$

## ■ Quark mass difference $m_u \neq m_d$ (negligible)

# Situation at ICHEP'06 / 08

$$a_{\mu}^{\text{had}} [\text{ee}] = (690.9 \pm 4.4) \times 10^{-10}$$

$$a_{\mu} [\text{ee}] = (11\,659\,180.5 \pm 4.4_{\text{had}} \pm 3.5_{\text{LBL}} \pm 0.2_{\text{QED+EW}}) \times 10^{-10}$$



$$\text{Hadronic HO} \quad - (9.8 \pm 0.1) \times 10^{-10}$$

$$\text{Hadronic LBL} \quad + (12.0 \pm 3.5) \times 10^{-10}$$

$$\text{Electroweak} \quad (15.4 \pm 0.2) \times 10^{-10}$$

$$\text{QED} \quad (11\,658\,471.9 \pm 0.1) \times 10^{-10}$$

Knecht-Nyffeler (2002), Melnikov-Vainhstein (2003)

Davier-Marciano (2004)

Kinoshita-Nio (2006)

Observed Difference with BNL using  $e^+e^-$ :

$$a_{\mu} [\text{exp}] - a_{\mu} [\text{SM}] = (27.5 \pm 8.4) \times 10^{-10}$$

➔ 3.3 „standard deviations“

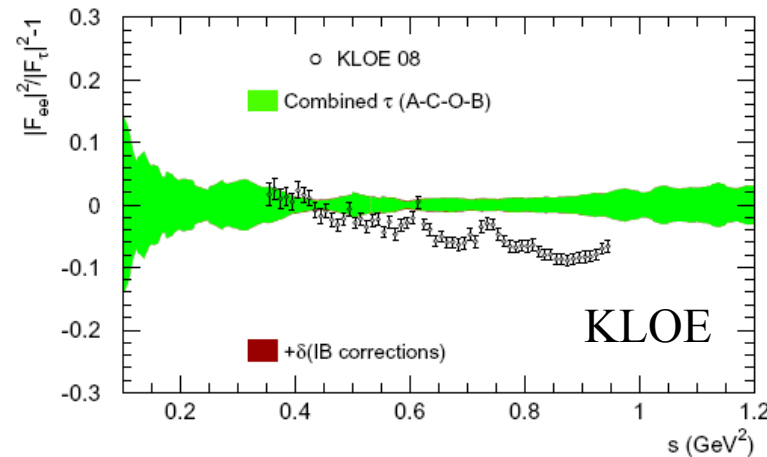
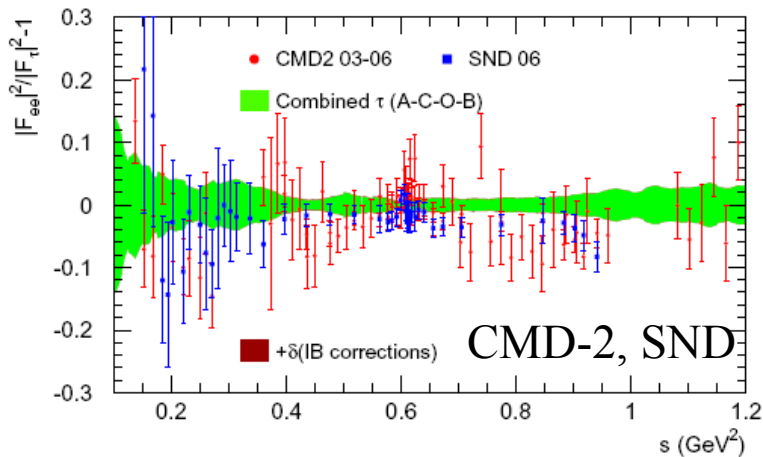
Estimate using  $\tau$  data consistent with E-821



# Revisited Analysis using $\tau$ Data: Belle + new IB

Relative comparison of  $\tau$  and ee spectral functions  
( $\tau$  green band)

arXiv:0906-5443 MD et al.

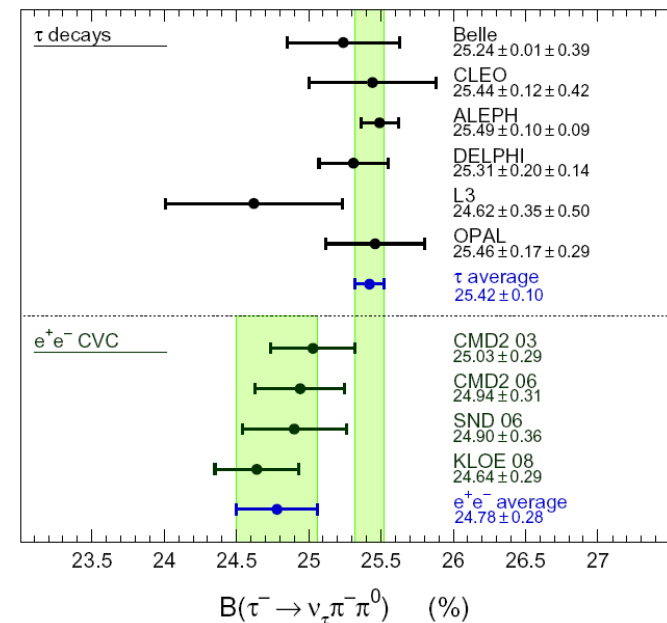


slope...

Global test of spectral functions:  
prediction of  $\tau$  BR using ee data

$$\mathcal{B}_X^{\text{CVC}} = \frac{3}{2} \frac{\mathcal{B}_e |V_{ud}|^2}{\pi \alpha^2 m_\tau^2} \int_{s_{\min}}^{m_\tau^2} ds s \sigma_{X^0}^I \left(1 - \frac{s}{m_\tau^2}\right)^2 \left(1 + \frac{2s}{m_\tau^2}\right)$$

$\Rightarrow$  larger disagreement with KLOE



# Goals of the BaBar Analysis

- ❖ Measure  $\sigma[e^+e^- \rightarrow \pi^+\pi^-(\gamma)]$  with high accuracy for vacuum polarization calculations, using the ISR method  $e^+e^- \rightarrow \pi^+\pi^-\gamma(\gamma)$
  - ❖  $\pi\pi$  channel contributes 73% of  $a_\mu^{\text{had}}$
  - ❖ Dominant uncertainty also from  $\pi\pi$
  - ❖ Also important to increase precision on  $\alpha(M_Z^2)$  (EW tests, ILC)
  - ❖ Present systematic precision of  $e^+e^-$  experiments
    - CMD-2 0.8%      SND 1.5%      in agreement
    - KLOE (ISR from 1.02 GeV) 2005 1.3%      some deviation in shape
    - 2008 0.9%      better agreement
  - ❖ Big advantage of ISR: all mass spectrum covered at once, from threshold to 3 GeV, with same detector and analysis
  - ❖ Measure simultaneously  $\pi^+\pi^-\gamma(\gamma)$  and  $\mu^+\mu^-\gamma(\gamma)$
  - ❖ Compare to spectral functions from previous  $e^+e^-$  data and  $\tau$  decays
- $\Rightarrow$  aim for a measurement with  $<1\%$  accuracy (syst. errors at per mil level)

great interest to clarify the situation as magnitude of possible discrepancy with SM is of the order of SUSY contributions with masses of a few 100 GeV

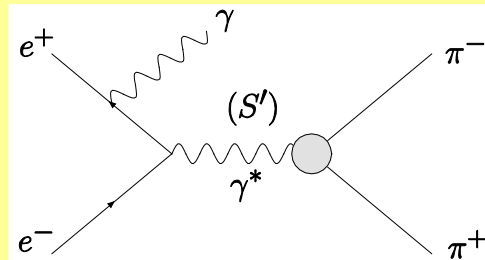
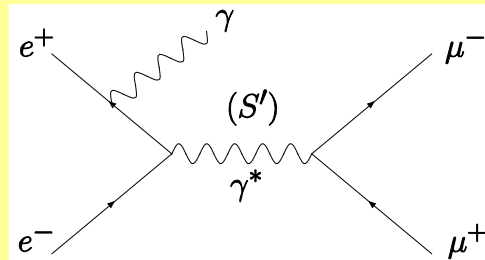
# The Relevant Processes

$e^+ e^- \rightarrow \mu^+ \mu^- \gamma (\gamma)$  and  $\pi^+ \pi^- \gamma (\gamma)$  measured simultaneously

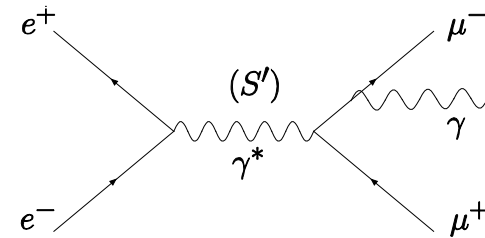
$$x = 2E_\gamma^*/\sqrt{s}$$

$$s' = s(1 - x)$$

ISR

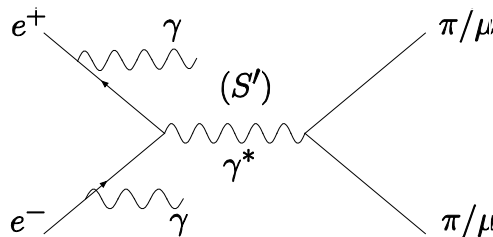


FSR

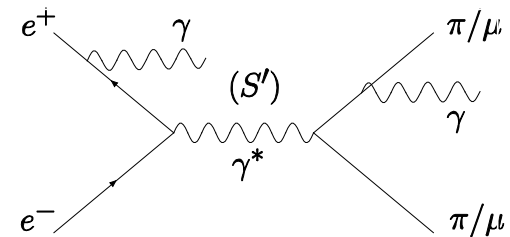


LO FSR negligible for  $\pi\pi$   
at  $s \sim (10.6 \text{ GeV})^2$

ISR + add. ISR



ISR + add. FSR



# BaBar / PEP II

- ❖ **PEP-II** is an asymmetric  $e^+e^-$  collider operating at CM energy of  $\Upsilon(4S)$ .
- ❖ Integrated luminosity =  $531 \text{ fb}^{-1}$

## BaBar EMC:

- 6580 CsI(Tl) crystals resolution  $\sim 1\text{-}2\%$  high E.

## BaBar IFR:

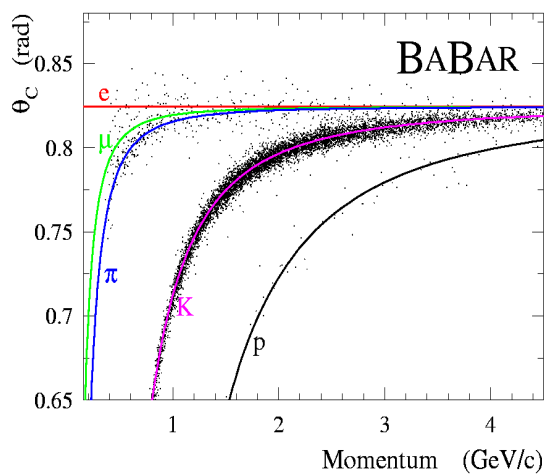
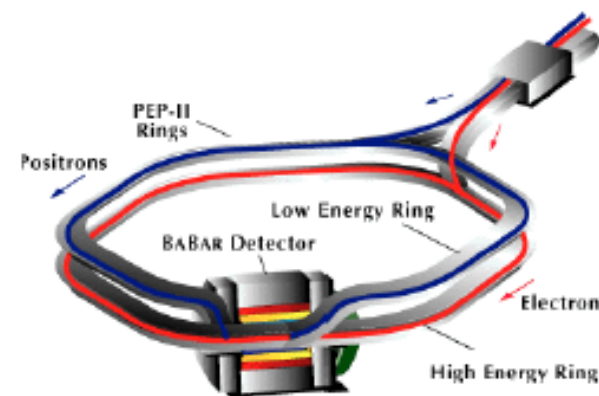
- resistive plate chambers

## BaBar DIRC

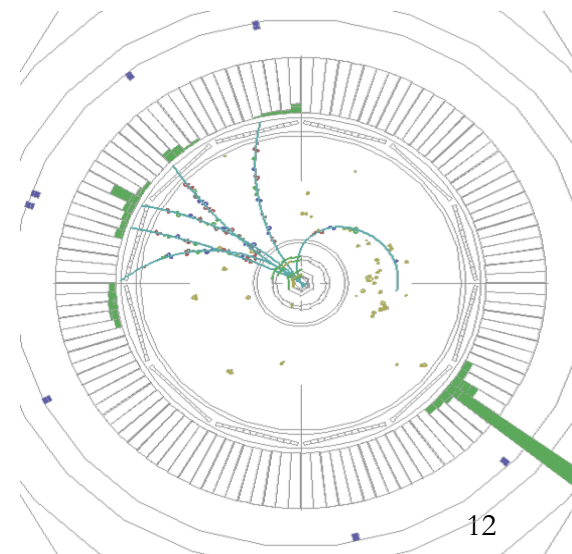
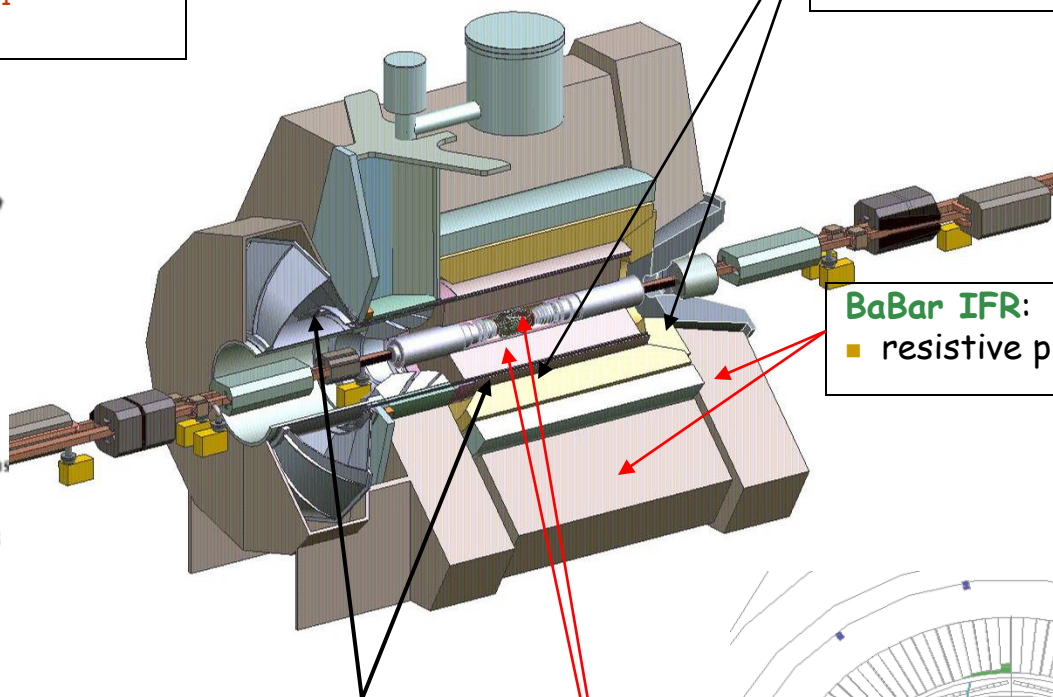
- particle ID up to  $4\text{-}5 \text{ GeV}/c$

## BaBar SVT and DCH

- precision tracking



M.Davies ISR  $\pi\pi/g-2$



Paris 6-7 7/10/2009

# Analysis Steps

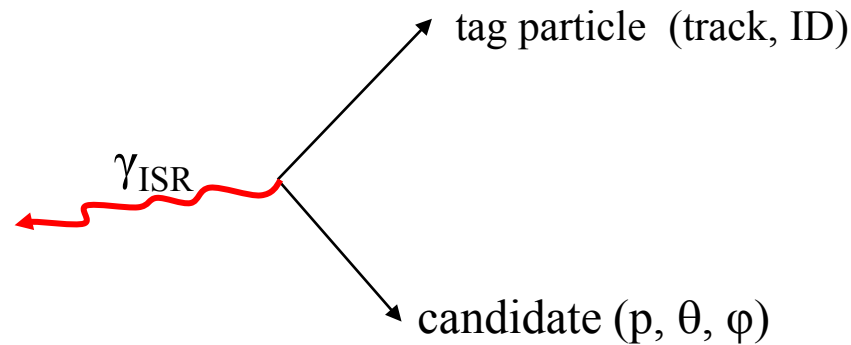
232 fb<sup>-1</sup> (Y(4S) on-peak & off peak)

- Measure ratio of  $\pi\pi\gamma(\gamma)$  to  $\mu\mu\gamma(\gamma)$  cross sections to cancel  $ee$  luminosity, additional ISR, vacuum polarization, ISR photon efficiency (otherwise 1-2% syst.)
- ISR photon at large angle in EMC + 2 tracks
  
- Geometrical acceptance (using Monte Carlo simulation)
- All efficiencies measured on data (data/MC corrections)
- Triggers (L1 hardware, L3 software), background-filter efficiencies
- Tracking efficiency
- Particle ID matrix (ID and mis-ID efficiencies):  $\mu$   $\pi$  K
- Kinematic fitting
  - reduce non 2-body backgrounds
  - $\chi^2$  cut efficiency: additional radiation (ISR, FSR), secondary interactions
- Unfolding of mass spectra
- Consistency checks for  $\mu\mu$  (QED test, ISR luminosity) and  $\pi\pi$
- Unblinding R  $\Rightarrow$  partial preliminary results (Tau08, Sept. 2008)
- Additional studies and checks
- Final results on  $\pi\pi$  cross section and calculation of dispersion integral

# MC Generators

- Acceptance and efficiencies determined initially from simulation, with data/MC corrections applied
- Large simulated samples, typically  $10 \times$  data, using AfkQed generator
- **AfkQed**: lowest-order (LO) QED with additional radiation:
  - ISR with structure function method,  $\gamma$  assumed collinear to the beams and with limited energy
  - FSR using PHOTOS
- **Phokhara 4.0**: (almost) exact second-order QED matrix element, limited to NLO
- Studies comparing Phokhara and AfkQed at 4-vector level with fast simulation
- QED test with  $\mu\mu\gamma$  ( $\gamma$ ) cross section requires reliable NLO generator
- $\pi\pi(\gamma)$  cross section obtained through  $\pi\pi\gamma / \mu\mu\gamma$  ratio, rather insensitive to detailed description of radiation in MC

# Particle-related Efficiency Measurements



- benefit from pair production for tracking and particle ID
- kinematically constrained events
- efficiency automatically averaged over running periods
- measurement in the same environment as for physics, in fact same events!
- applied to particle ID with  $\pi/K/\mu$  samples, tracking, study of secondary interactions...
- assumes that efficiencies of the 2 particles are uncorrelated
- in practice not true  $\Rightarrow$  study of 2-particle overlap in the detector (trigger, tracking, EMC, IFR) required a large effort to reach per mil accuracies

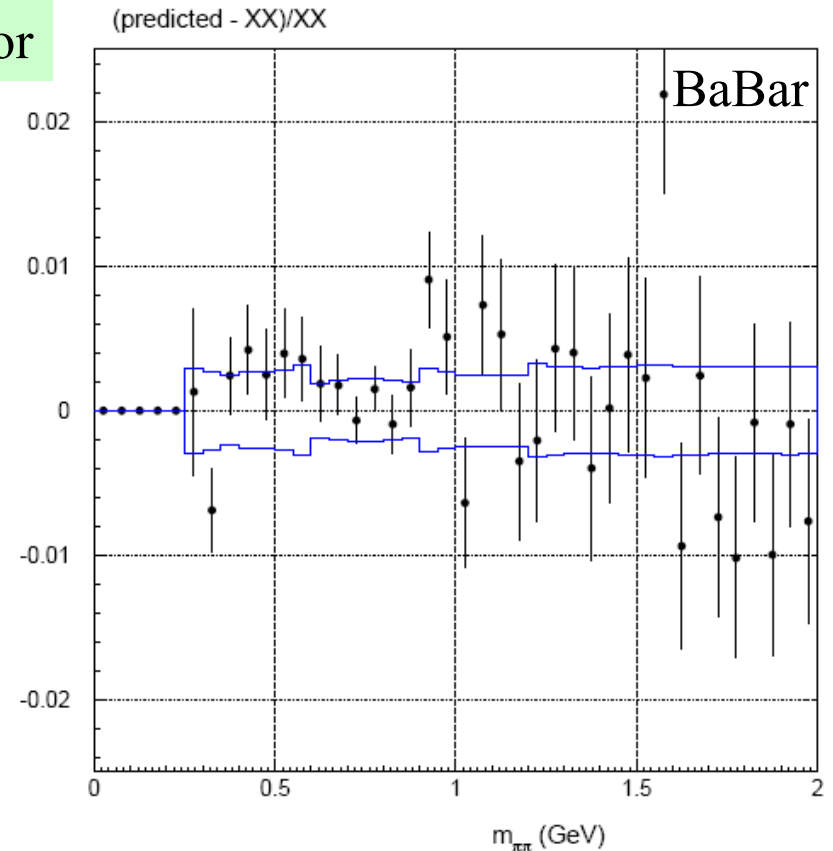
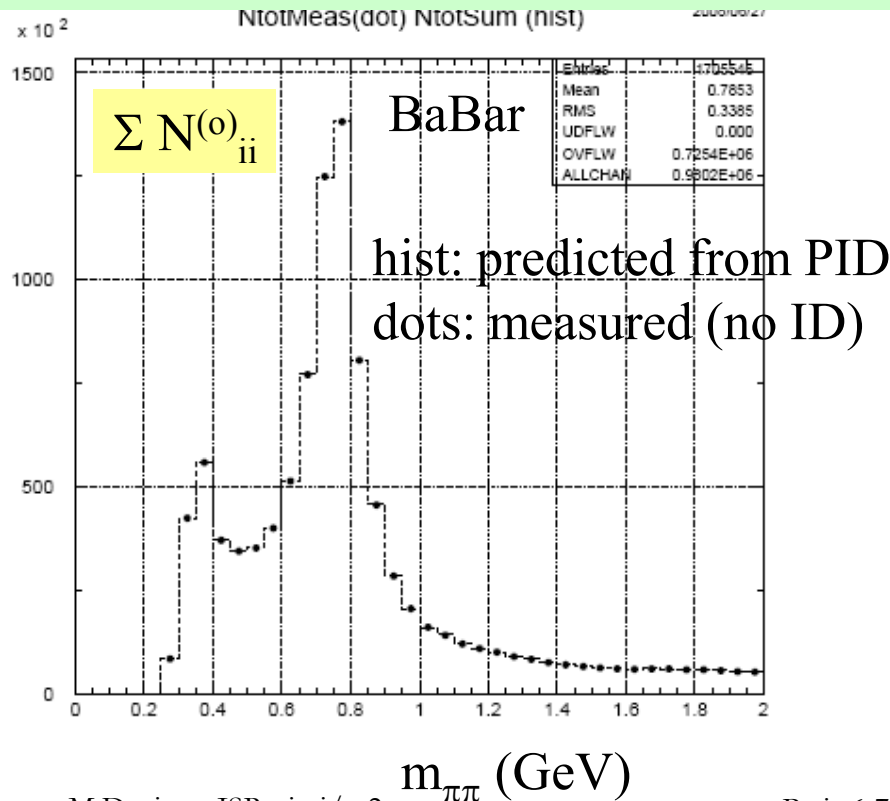
# PID separation and Global Test

$$N_{\pi\pi'} = N_{\mu\mu}^{(0)} \varepsilon_{\mu\mu \rightarrow \pi\pi'} + N_{\pi\pi}^{(0)} \varepsilon_{\pi\pi \rightarrow \pi\pi'} + N_{KK}^{(0)} \varepsilon_{KK \rightarrow \pi\pi'} + N_{ee/\pi\pi'}$$

$$N_{\mu\mu'} = N_{\mu\mu}^{(0)} \varepsilon_{\mu\mu \rightarrow \mu\mu'} + N_{\pi\pi}^{(0)} \varepsilon_{\pi\pi \rightarrow \mu\mu'} + N_{KK}^{(0)} \varepsilon_{KK \rightarrow \mu\mu'}$$

$$N_{KK'} = N_{\mu\mu}^{(0)} \varepsilon_{\mu\mu \rightarrow KK'} + N_{\pi\pi}^{(0)} \varepsilon_{\pi\pi \rightarrow KK'} + N_{KK}^{(0)} \varepsilon_{KK \rightarrow KK'}$$

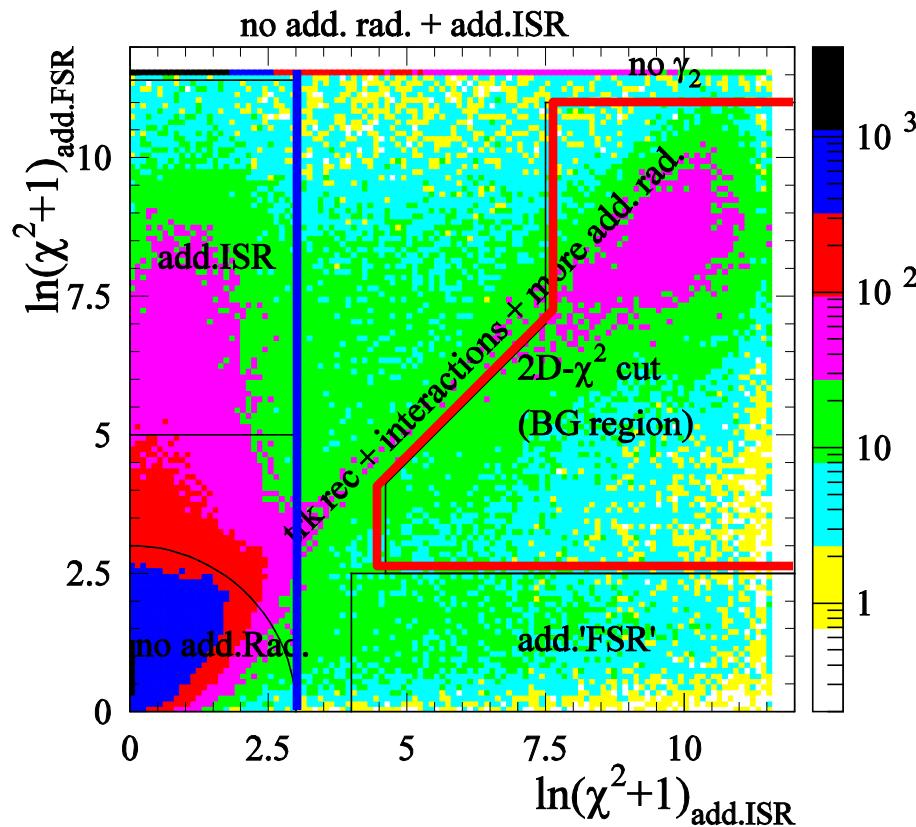
All 'xx'  $\Rightarrow$  solve for all  $xx^{(0)}$  and compare with no-ID spectrum and estimated syst. error





# Kinematic Fitting

$\pi\pi\gamma(\gamma)$



- Two kinematic fits to  $X X \gamma_{\text{ISR}} \gamma_{\text{add}}$   
(ISR photon defined as highest energy)

Add. ISR fit:  $\gamma_{\text{add}}$  assumed along beams

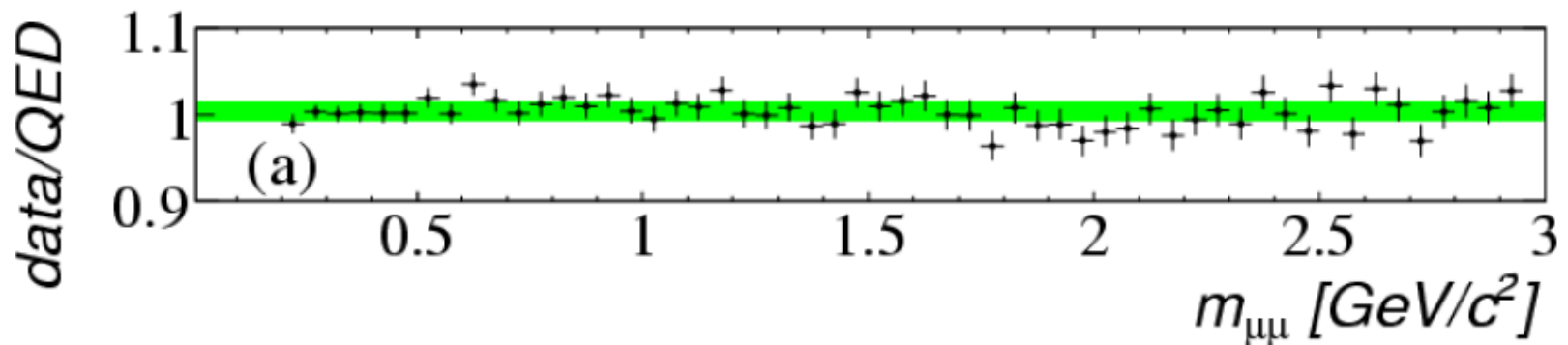
Add. 'FSR' if  $\gamma_{\text{add}}$  detected

- First analysis to measure cross section with additional photons (NLO)
- Loose  $\chi^2$  cut (outside BG region in plot) for  $\mu\mu$  and  $\pi\pi$  in central  $\rho$  region
- Tight  $\chi^2$  cut ( $\ln(\chi^2+1) < 3$ ) for  $\pi\pi$  in  $\rho$  tail region
- $q \bar{q}$  and multi-hadronic ISR background from MC samples + normalization from data using signals from  $\pi^0 \rightarrow \gamma_{\text{ISR}} \gamma$  ( $q\bar{q}$ ), and  $\omega$  and  $\phi$  ( $\pi\pi\pi^0\gamma$ )

# QED Test with $\mu\mu\gamma$ sample

- absolute comparison of  $\mu\mu$  mass spectra in data and in simulation
- simulation corrected for data/MC efficiencies
- AfkQed corrected for incomplete NLO using Phokhara
- strong test (ISR probability drops out for  $\pi\pi$ )

BaBar



$$\frac{\sigma_{\mu\mu\gamma(\gamma)}^{\text{data}}}{\sigma_{\mu\mu\gamma(\gamma)}^{\text{NLO QED}}} = 1 + (4.0 \pm 1.9 \pm 5.5 \pm 9.4) 10^{-3} \quad (0.2 - 3 \text{ GeV})$$

ISR  $\gamma$  efficiency 3.4 syst.  
trig/track/PID 4.0

BaBar ee luminosity

# Obtaining the $\pi\pi(\gamma)$ cross section

$$\frac{dN_{\pi\pi\gamma(\gamma)}}{d\sqrt{s'}} = \frac{dL_{ISR}^{eff}}{d\sqrt{s'}} \varepsilon_{\pi\pi\gamma(\gamma)}(\sqrt{s'}) \sigma_{\pi\pi(\gamma)}^0(\sqrt{s'})$$

Unfolded spectrum

Acceptance from MC + data/MC corrections

Effective ISR luminosity from  $\mu\mu\gamma(\gamma)$  analysis (similar equation + QED)

$\pi\pi$  mass spectrum unfolded (Malaescu arXiv:0907-3791) for detector response

Additional ISR almost cancels in the procedure ( $\pi\pi\gamma(\gamma) / \mu\mu\gamma(\gamma)$  ratio)

Correction  $(2.5 \pm 1.0) 10^{-3} \Rightarrow \pi\pi$  cross section does not rely on accurate description of NLO in the MC generator

ISR luminosity from  $\mu\mu\gamma\gamma$  in 50-MeV energy intervals  
(small compared to variation of efficiency corrections)

# Systematic uncertainties

$\sqrt{s}$  intervals (GeV)

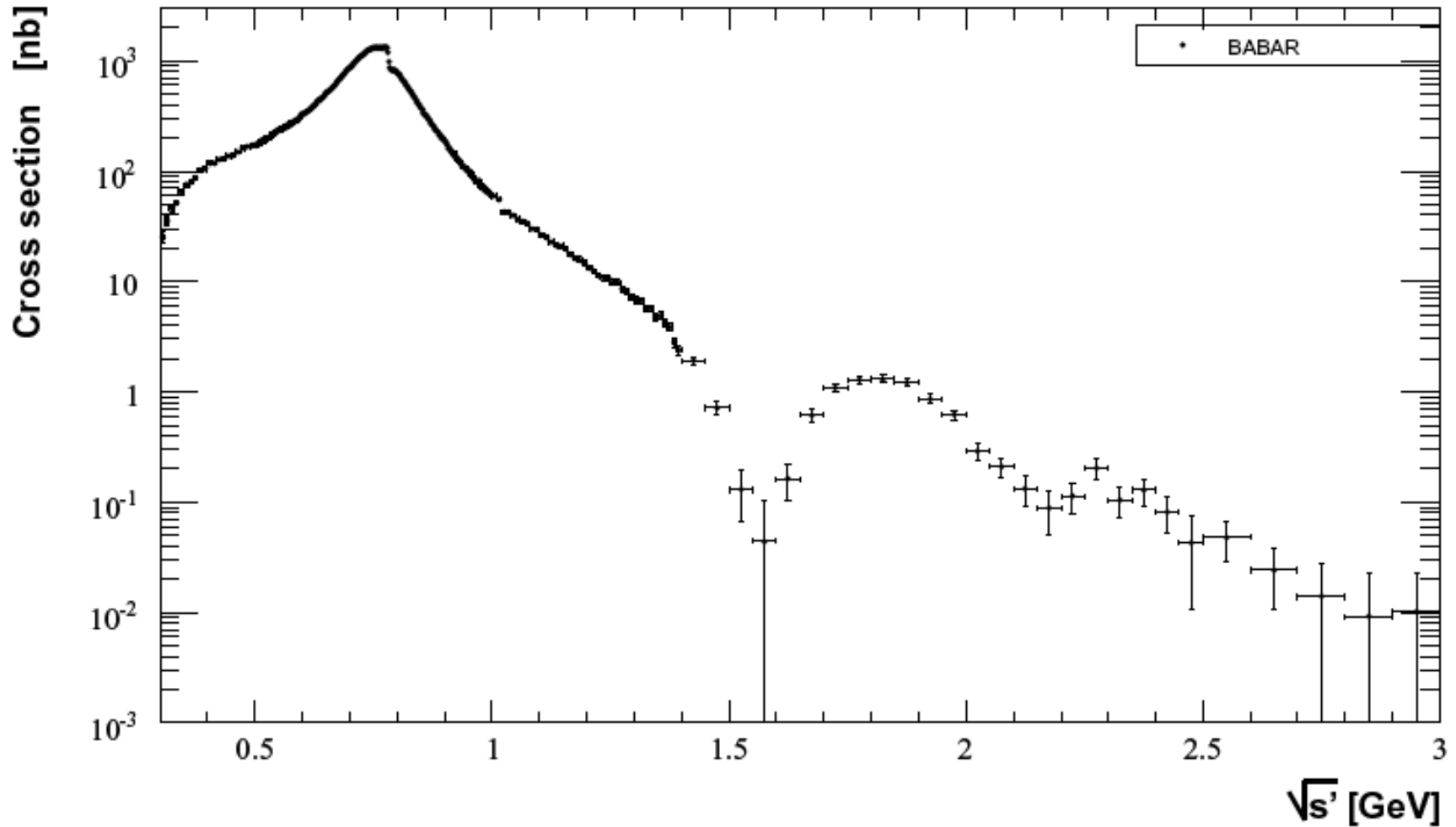
errors in  $10^{-3}$

sources	0.3-0.4	0.4-0.5	0.5-0.6	0.6-0.9	0.9-1.2	1.2-1.4	1.4-2.0	2.0-3.0
trigger/ filter	5.3	2.7	1.9	1.0	0.5	0.4	0.3	0.3
tracking	3.8	2.1	2.1	1.1	1.7	3.1	3.1	3.1
$\pi$ -ID	10.1	2.5	6.2	2.4	4.2	10.1	10.1	10.1
background	3.5	4.3	5.2	1.0	3.0	7.0	12.0	50.0
acceptance	1.6	1.6	1.0	1.0	1.6	1.6	1.6	1.6
kinematic fit ( $\chi^2$ )	0.9	0.9	0.3	0.3	0.9	0.9	0.9	0.9
correl $\mu\mu$ ID loss	3.0	2.0	3.0	1.3	2.0	3.0	10.0	10.0
$\pi\pi/\mu\mu$ cancel.	2.7	1.4	1.6	1.1	1.3	2.7	5.1	5.1
unfolding	1.0	2.7	2.7	1.0	1.3	1.0	1.0	1.0
ISR luminosity	3.4	3.4	3.4	3.4	3.4	3.4	3.4	3.4
sum (cross section)	13.8	8.1	10.2	5.0	6.5	13.9	19.8	52.4

Dominated by particle ID ( $\pi$ -ID, correlated  $\mu\mu \rightarrow \pi\pi$ ,  $\mu$ -ID in ISR luminosity)

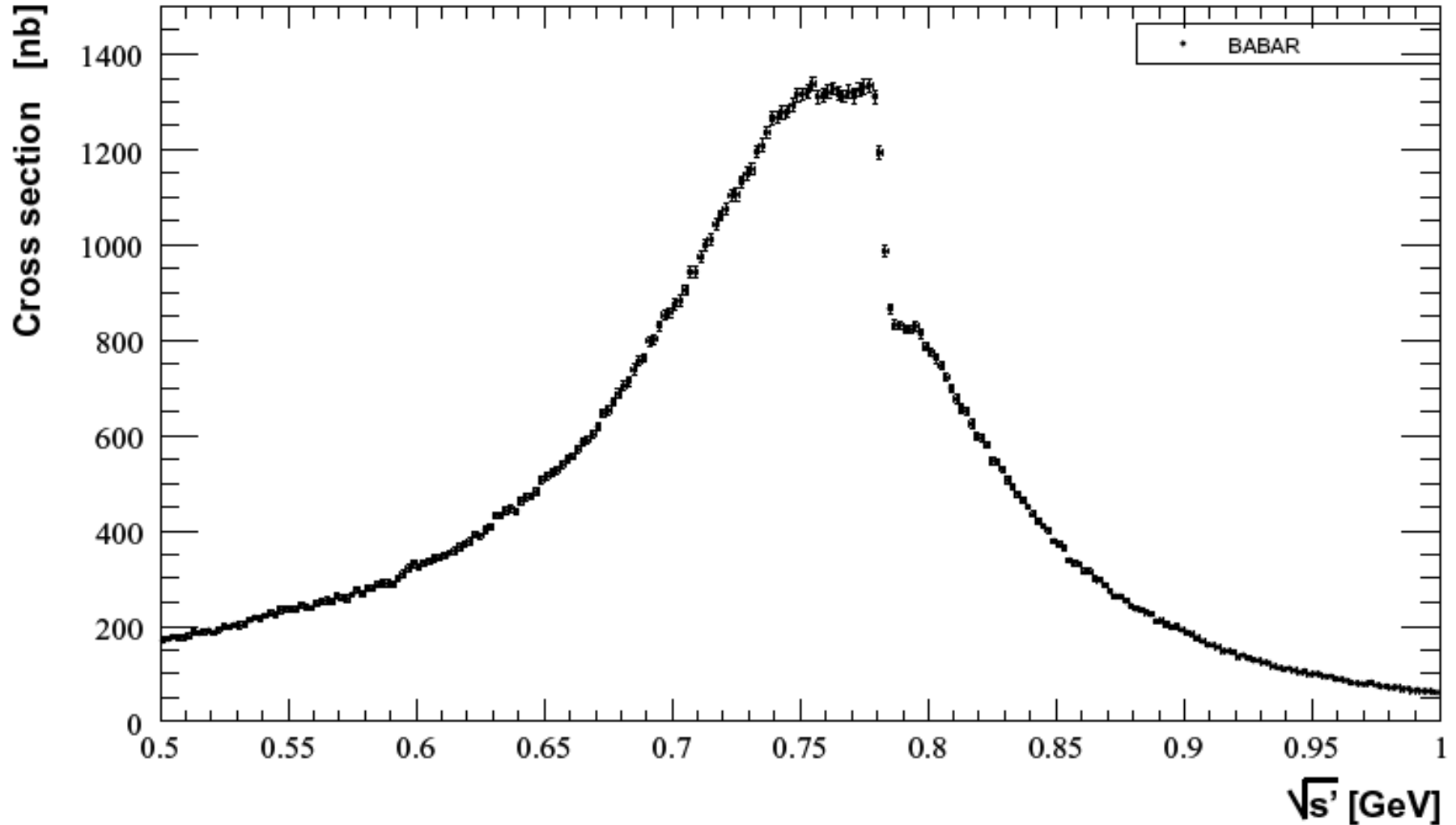
# BaBar results (arXiv:0908.3589)

$e^+ e^- \rightarrow \pi^+ \pi^- (\gamma)$     bare (no VP) cross section    diagonal errors stat+syst



# BaBar results in $\rho$ region

2-MeV energy intervals



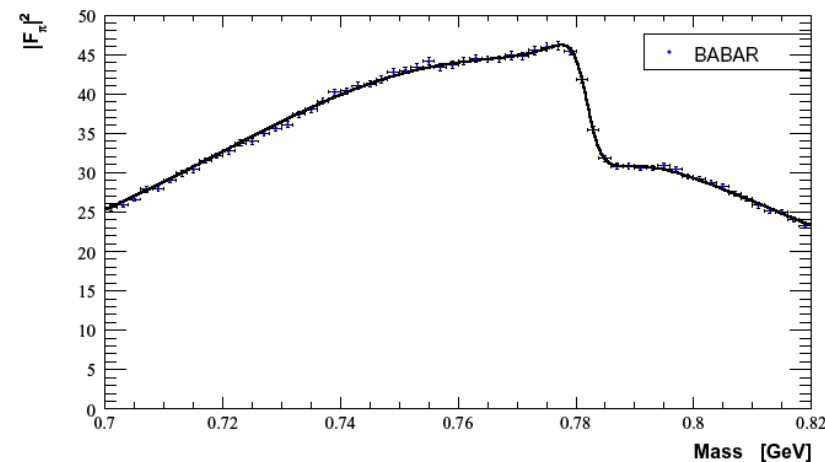
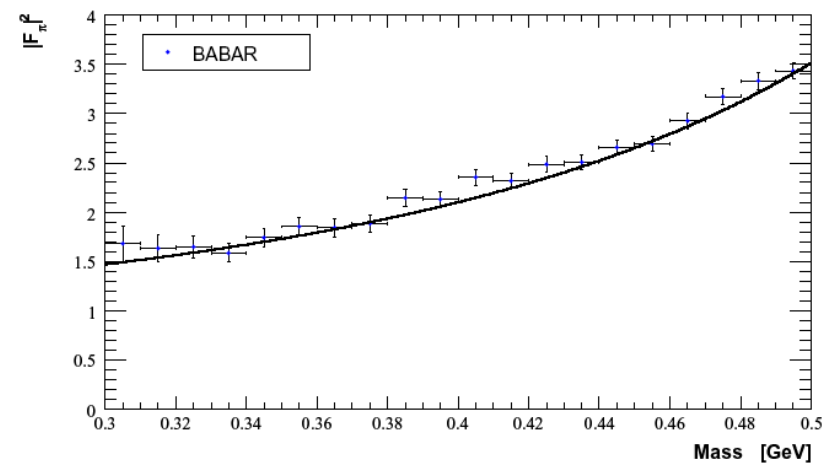
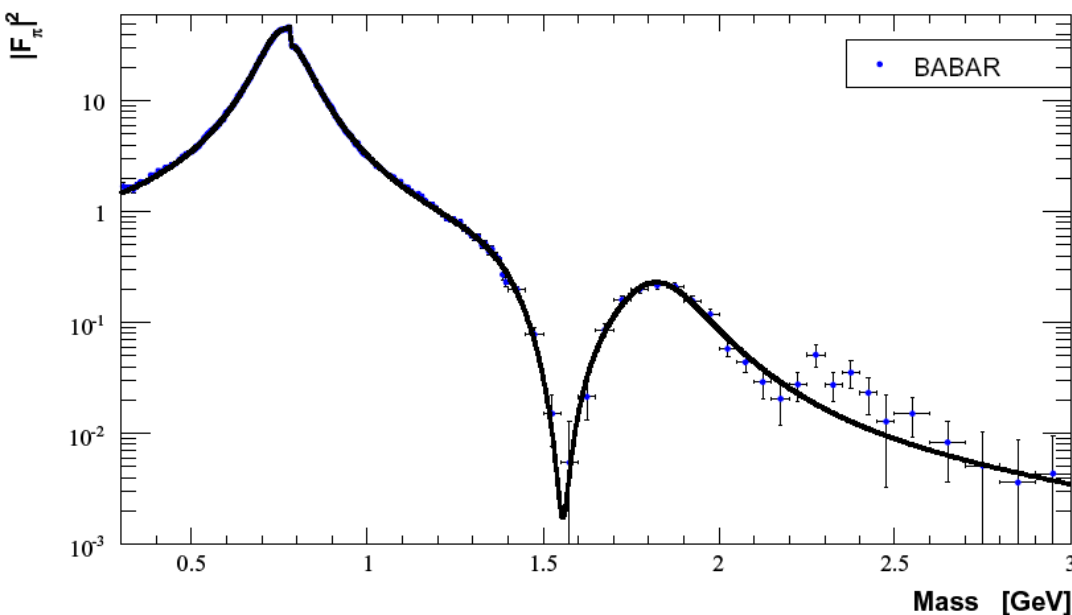
# VDM fit of the pion form factor

$$F_{\pi}(s) = \frac{BW_{\rho}^{GS}(s, m_{\rho}, \Gamma_{\rho}) \frac{1 + \alpha BW_{\omega}^{KS}(s, m_{\omega}, \Gamma_{\omega})}{1 + \alpha} + \beta BW_{\rho'}^{GS}(s, m_{\rho'}, \Gamma_{\rho'}) + \gamma BW_{\rho''}^{GS}(s, m_{\rho''}, \Gamma_{\rho''})}{1 + \beta + \gamma}$$

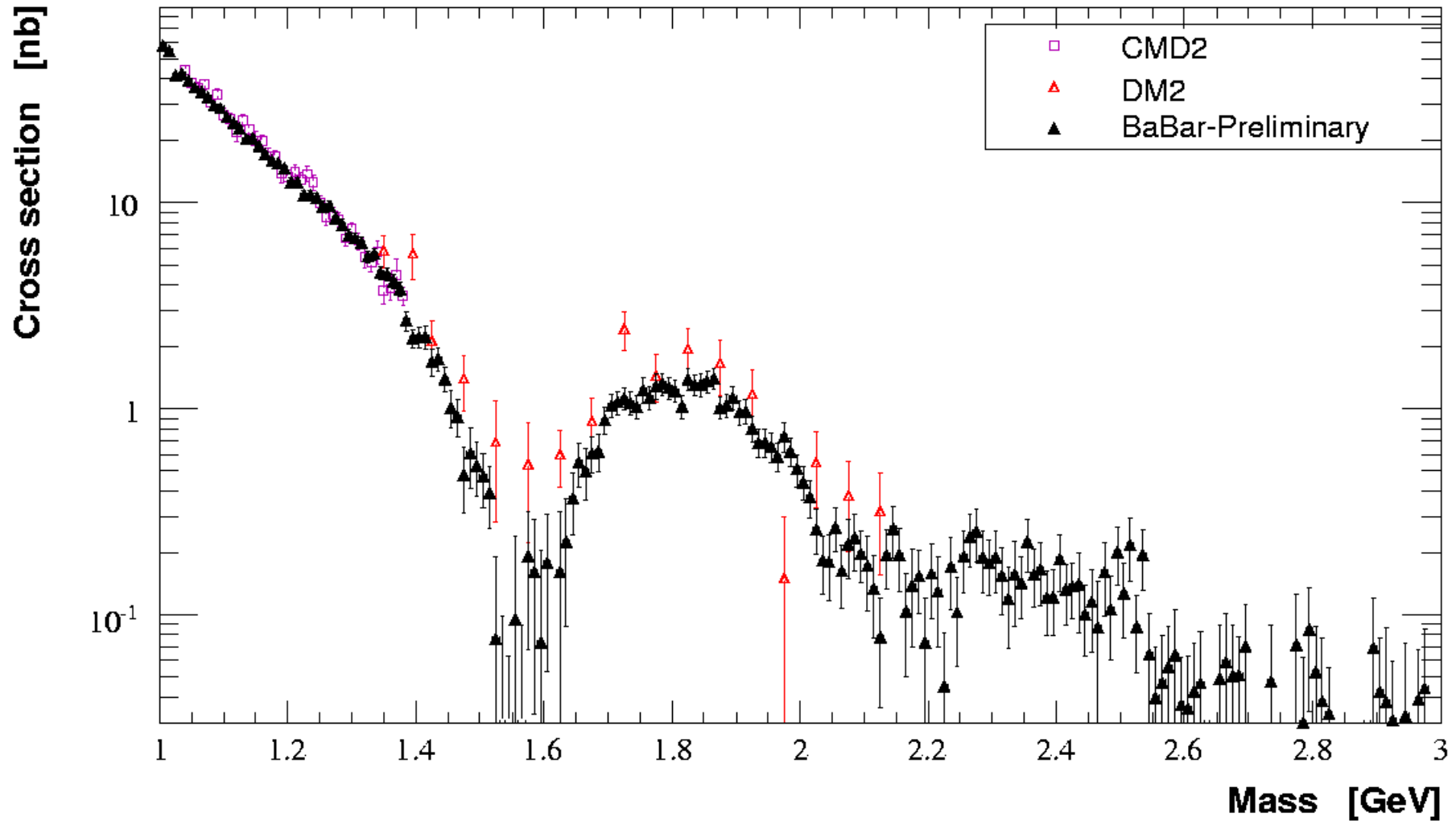
$$|F_{\pi}|^2(s') = \frac{3s'}{\pi\alpha^2(0)\beta_{\pi}^3} \sigma_{\pi\pi}(s')$$

$$\sigma_{\pi\pi}(s') = \frac{\sigma_{\pi\pi(\gamma)}^0(s')}{1 + \frac{\alpha}{\pi}\eta(s')} \left( \frac{\alpha(s')}{\alpha(0)} \right)^2$$

add. FSR      $\alpha$  Running (VP)



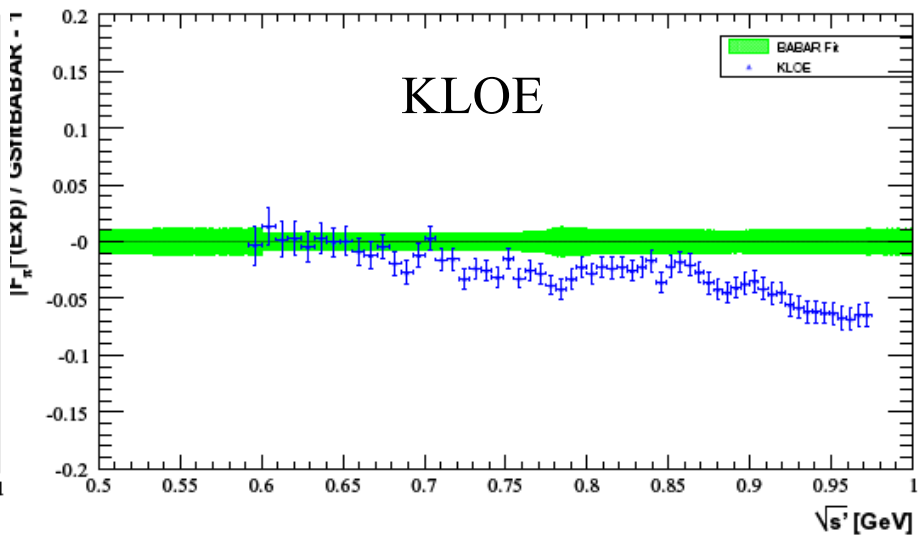
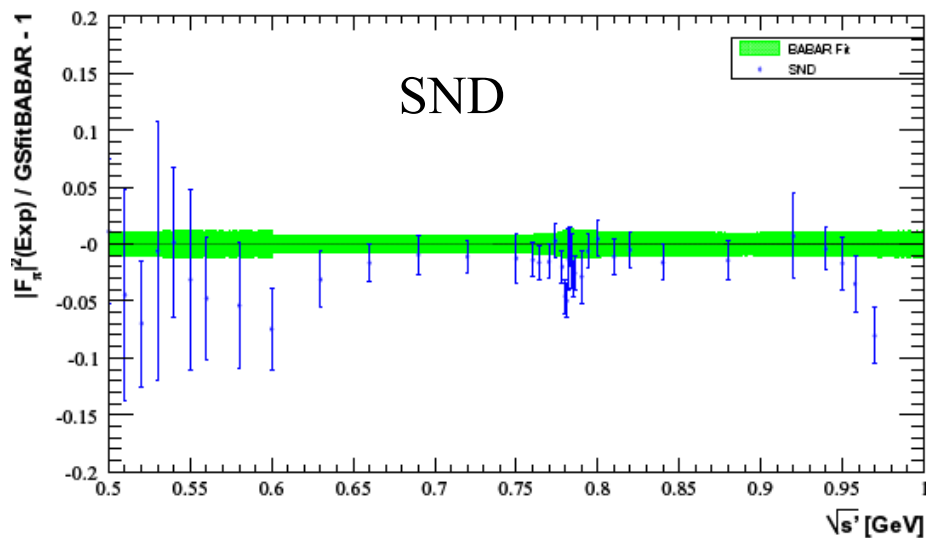
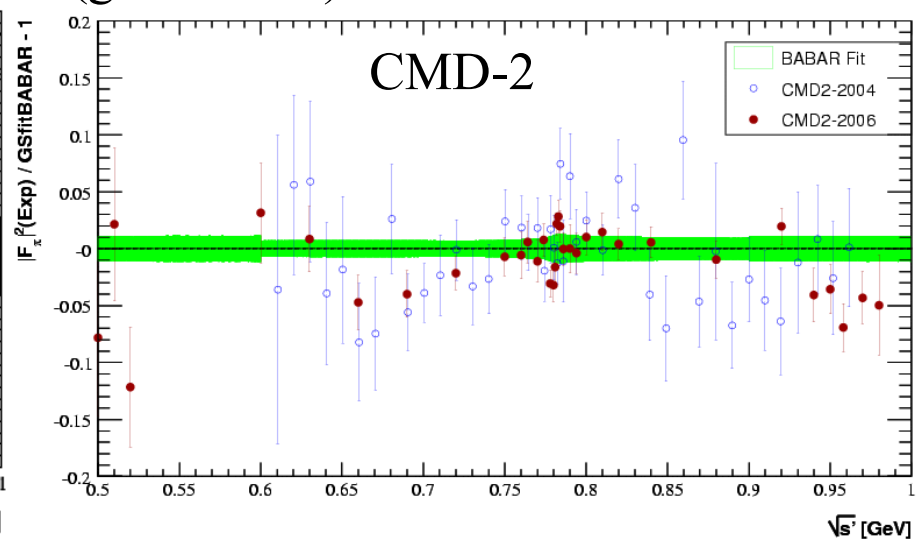
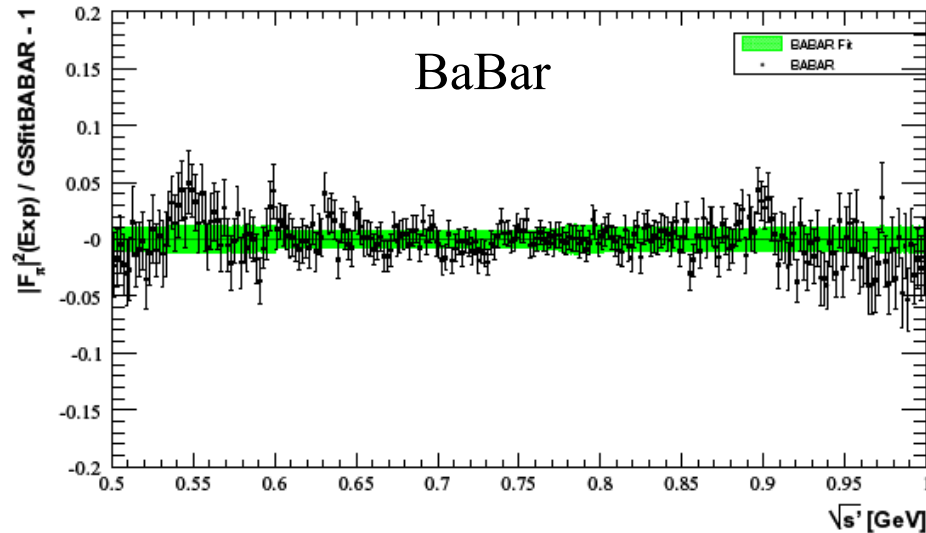
# BaBar vs. other experiments at larger mass



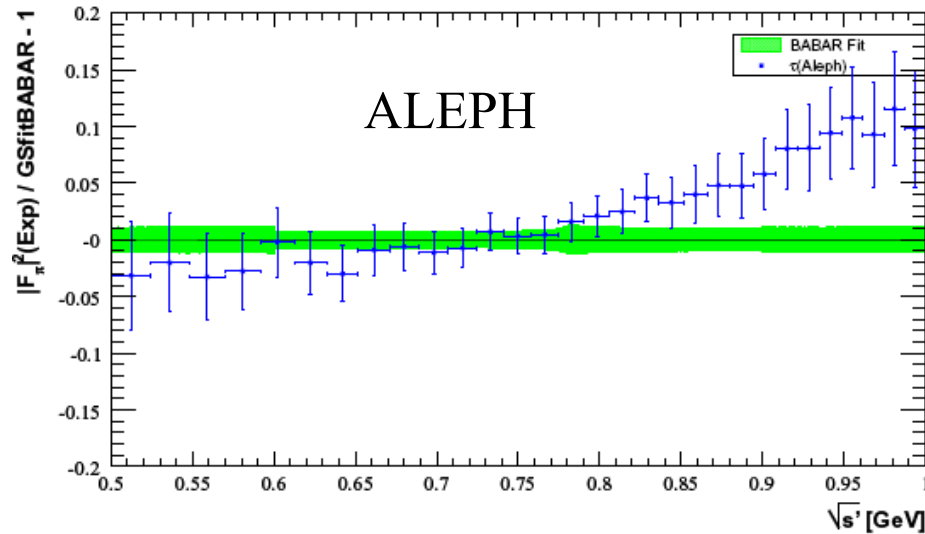


# BaBar vs. other ee data (0.5-1.0 GeV)

direct relative comparison of cross sections with BaBar fit (stat + syst errors included)  
(green band)



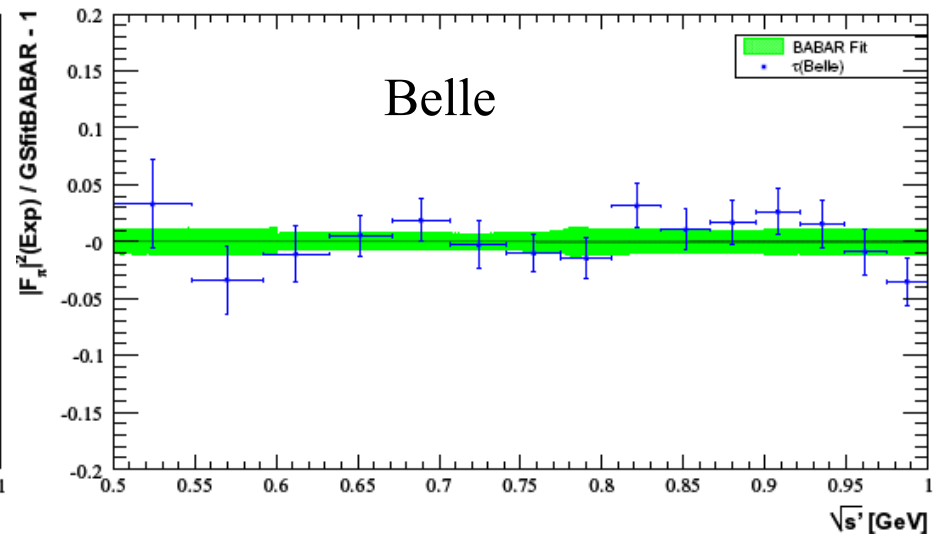
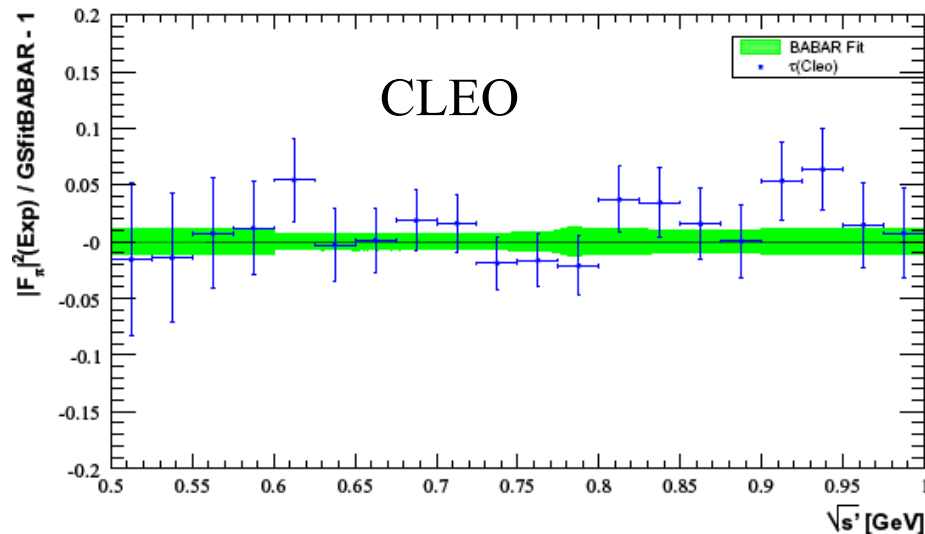
# BaBar vs. IB-corrected $\tau$ data (0.5-1.0 GeV)



relative comparison w.r.t. BaBar of isospin-breaking corrected  $\tau$  spectral functions

IB corrections: radiative corr.,  $\pi$  masses,  $\rho$ - $\omega$  interference,  $\rho$  masses/widths

each  $\tau$  data normalized to its own BR



# Computing $a_\mu^{\pi\pi}$

$$a_\mu^{\pi\pi(\gamma),LO} = \frac{1}{4\pi^3} \int_{4m_\pi^2}^{\infty} ds K(s) \sigma_{\pi\pi(\gamma)}^0(s) ,$$

where  $K(s)$  is the QED kernel,

$$K(s) = x^2 \left(1 - \frac{x^2}{2}\right) + (1+x)^2 \left(1 + \frac{1}{x^2}\right) \left[ \ln(1+x) - x + \frac{x^2}{2} \right] + x^2 \frac{1+x}{1-x} \ln x ,$$

with  $x = (1 - \beta_\mu)/(1 + \beta_\mu)$  and  $\beta_\mu = (1 - 4m_\mu^2/s)^{1/2}$ .

$m_{\pi\pi}$ range (GeV)	$a_\mu^{\pi\pi(\gamma),LO}$ BABAR
0.28–0.30	$0.55 \pm 0.01 \pm 0.01$
0.30–0.50	$57.62 \pm 0.63 \pm 0.55$
0.50–1.00	$445.94 \pm 2.10 \pm 2.51$
1.00–1.80	$9.97 \pm 0.10 \pm 0.09$
0.28–1.80	$514.09 \pm 2.22 \pm 3.11$

( $\times 10^{-10}$ )

0.28–1.8 (GeV)

**BABAR**

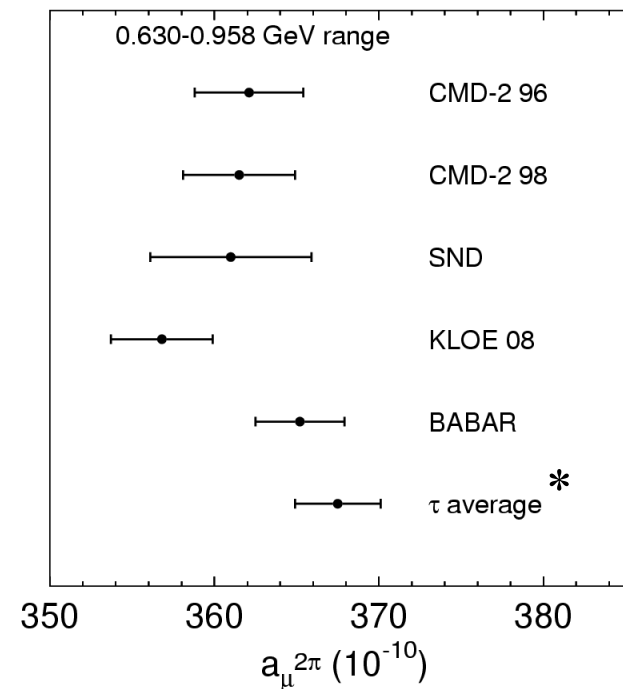
**$514.1 \pm 3.8$**

previous  $e^+e^-$  combined

**$503.5 \pm 3.5$  \***

$\tau$  combined

**$515.2 \pm 3.5$  \***



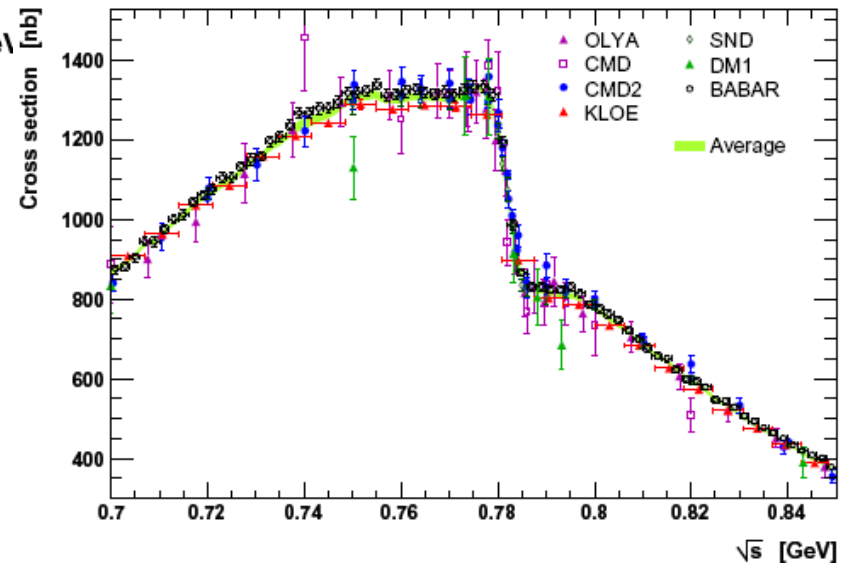
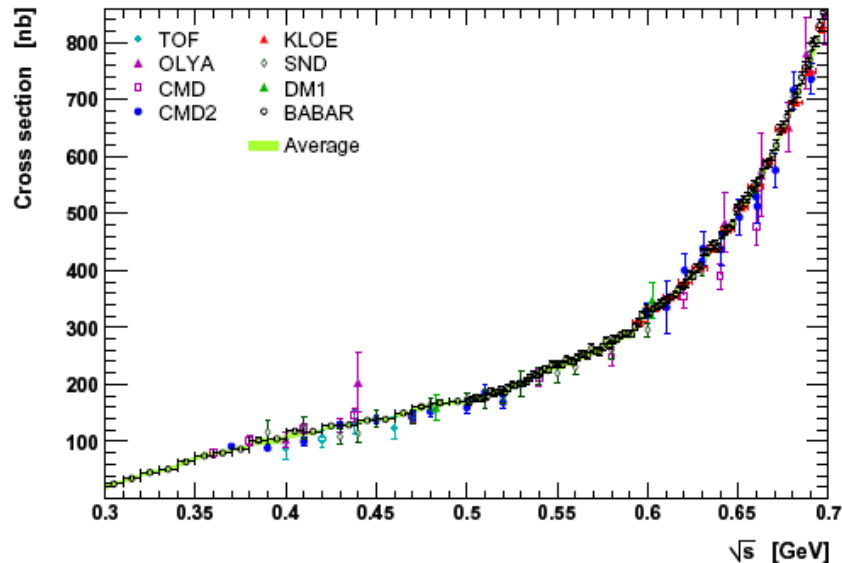
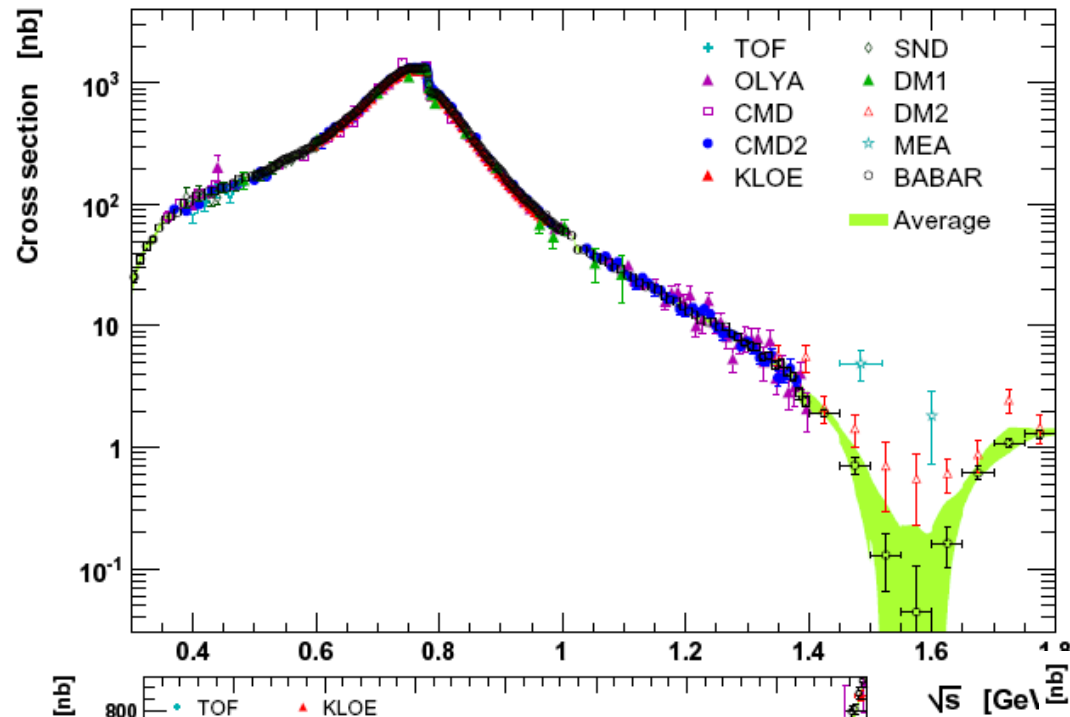
\* arXiv:0906-5443 MD et al.

# Including BaBar in the $e^+e^-$ Combination

arXiv: 0908.4300

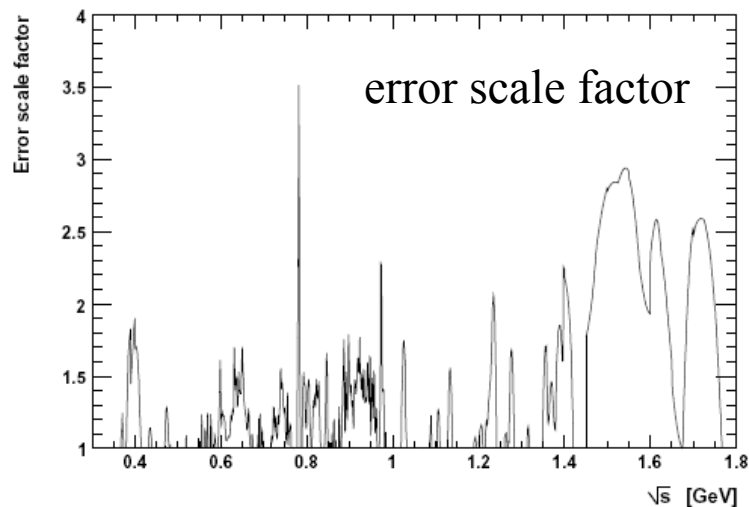
MD-Hoecker-Malaescu-Yuan-Zhang

Improved procedure and software (HVPTools) for combining cross section data with arbitrary point spacing/binning

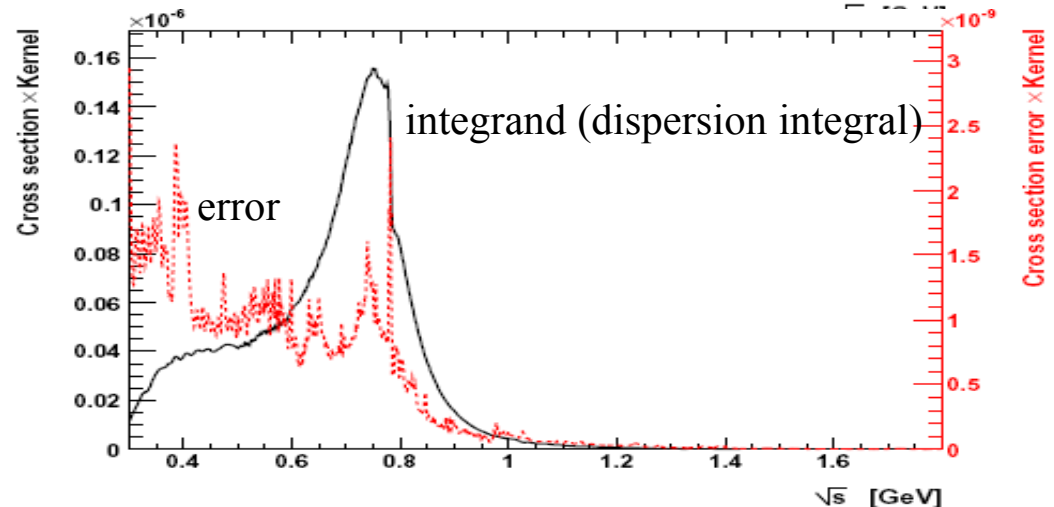
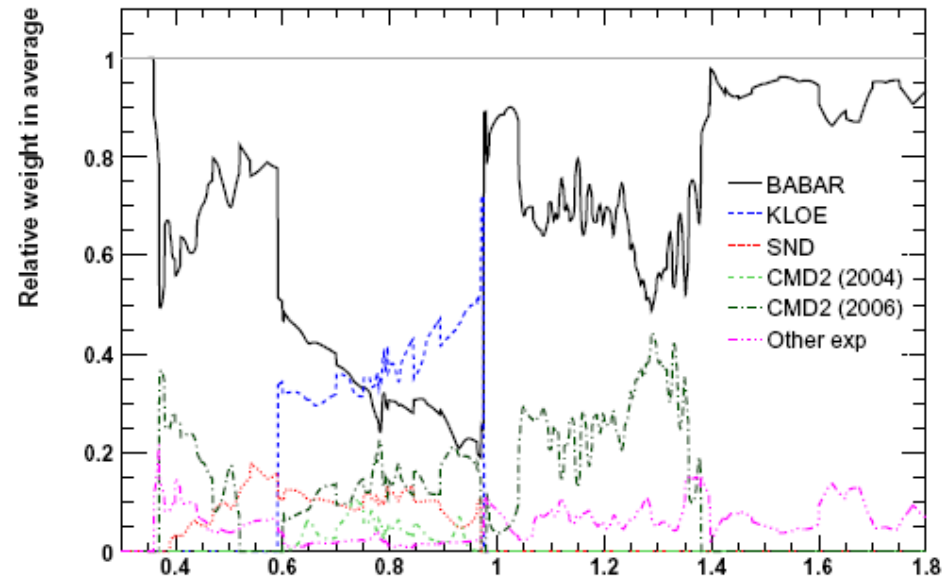


# Obtaining the average cross section

- local weighted average performed
- full covariance matrices
- local  $\chi^2$  used for error rescaling
- average dominated by BaBar and KLOE, BaBar covering full range



relative weights



# Other hadronic contributions

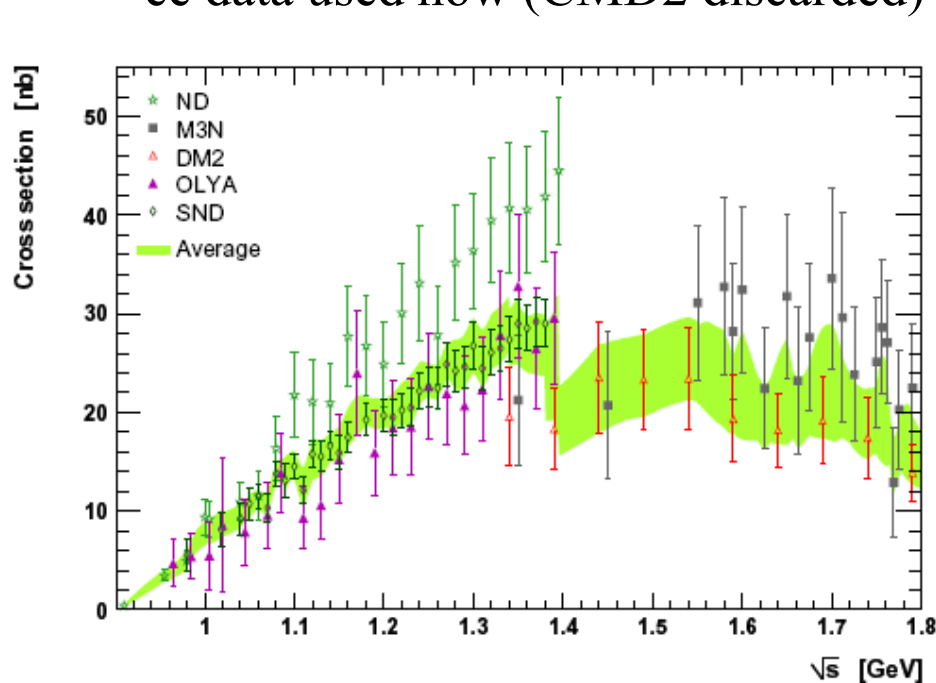
from MD-Eidelman-Hoecker-Zhang (2006)

Modes	Energy [GeV]	$e^+e^-$	$\tau$
$\pi^+\pi^-2\pi^0$	$2m_\pi - 1.8$	$16.8 \pm 1.3 \pm 0.2_{\text{rad}}$	$21.4 \pm 1.3 \pm 0.6_{\text{SU}(2)}$
$2\pi^+2\pi^- (+\text{BaBar})$	$2m_\pi - 1.8$	$13.1 \pm 0.4 \pm 0.0_{\text{rad}}$	$12.3 \pm 1.0 \pm 0.4_{\text{SU}(2)}$
$\omega (782)$	$0.3 - 0.81$	$38.0 \pm 1.0 \pm 0.3_{\text{rad}}$	—
$\phi (1020)$	$1.0 - 1.055$	$35.7 \pm 0.8 \pm 0.2_{\text{rad}}$	—
Other excl. (+BaBar)	$2m_\pi - 1.8$	$24.3 \pm 1.3 \pm 0.2_{\text{rad}}$	—
$J/\psi, \psi(2S)$	$3.08 - 3.11$	$7.4 \pm 0.4 \pm 0.0_{\text{rad}}$	—
$R [\text{QCD}]$	$1.8 - 3.7$	$33.9 \pm 0.5_{\text{theo}}$	—
$R [\text{data}]$	$3.7 - 5.0$	$7.2 \pm 0.3 \pm 0.0_{\text{rad}}$	—
$R [\text{QCD}]$	$5.0 - \infty$	$9.9 \pm 0.2_{\text{theo}}$	—

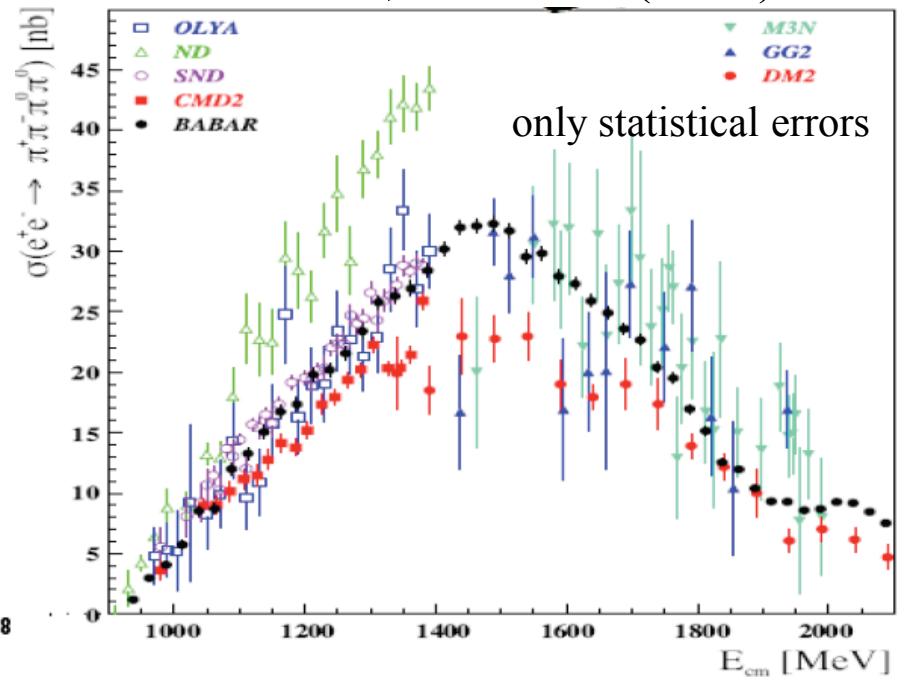
$\Rightarrow$  another large long-standing discrepancy in the  $\pi^+\pi^-2\pi^0$  channel !

# The Problematic $2\pi\ 2\pi^0$ Contribution

ee data used now (CMD2 discarded)

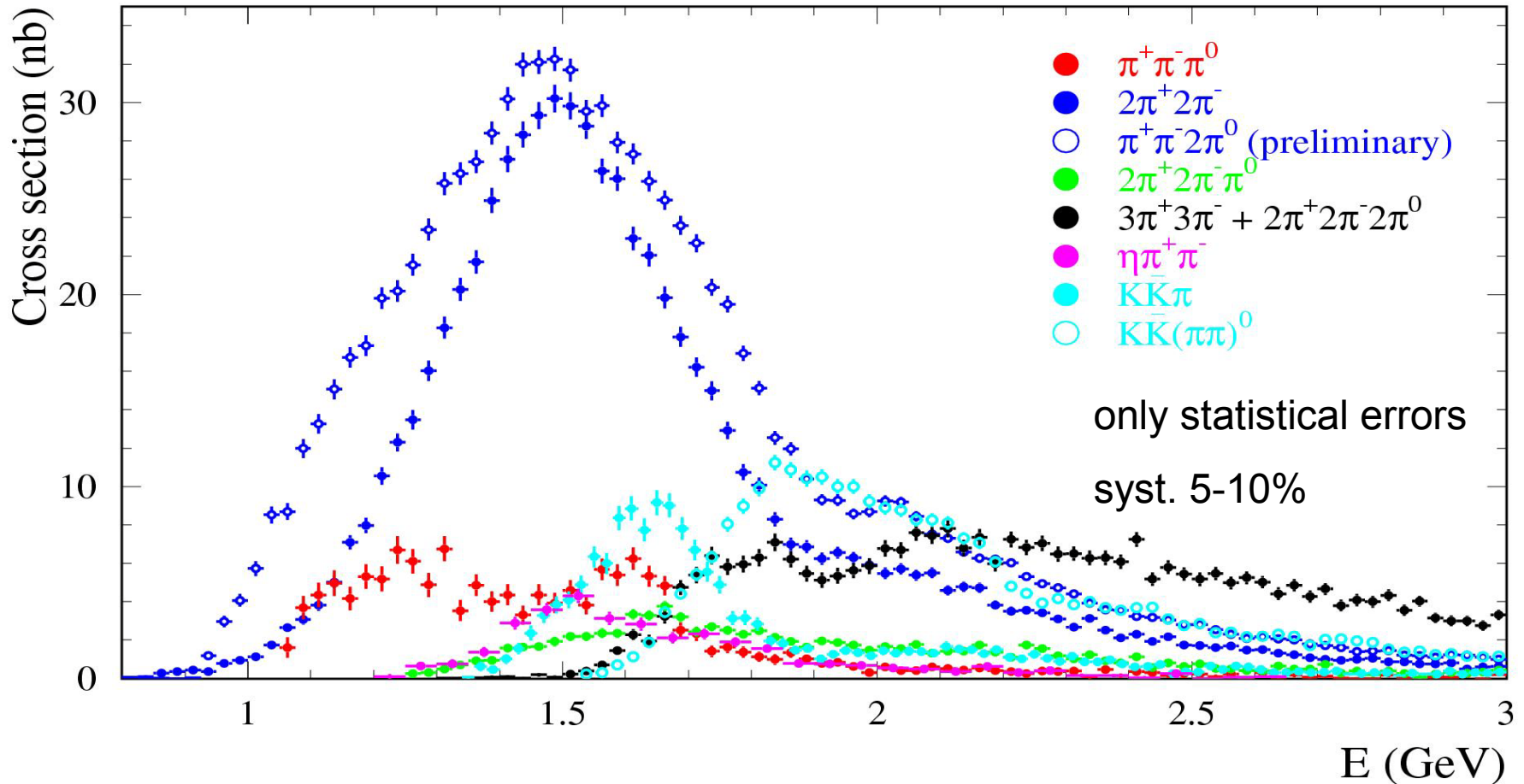


preliminary BaBar data:  
A. Petzold, EPS-HEP (2007)



old contribution	$16.8 \pm 1.3$	
update	$17.6 \pm 1.7$	probably still underestimated (BaBar)
$\tau$	$21.4 \pm 1.4$	

# BaBar Multi-hadronic Results



Still more channels under analysis:  $K^+K^-$ ,  $KK\pi\pi$  with  $K^0$



# Where are we?

- including BaBar  $2\pi$  results in the  $e^+e^-$  combination + estimate of hadronic LBL contribution (Prades-de Rafael-Vainhstein, 2009) yields

$$a_\mu^{\text{SM}}[e^+e^-] = (11\,659\,183.4 \pm 4.1 \pm 2.6 \pm 0.2) 10^{-10}$$

HVP LBL EW ( $\pm 4.9$ )

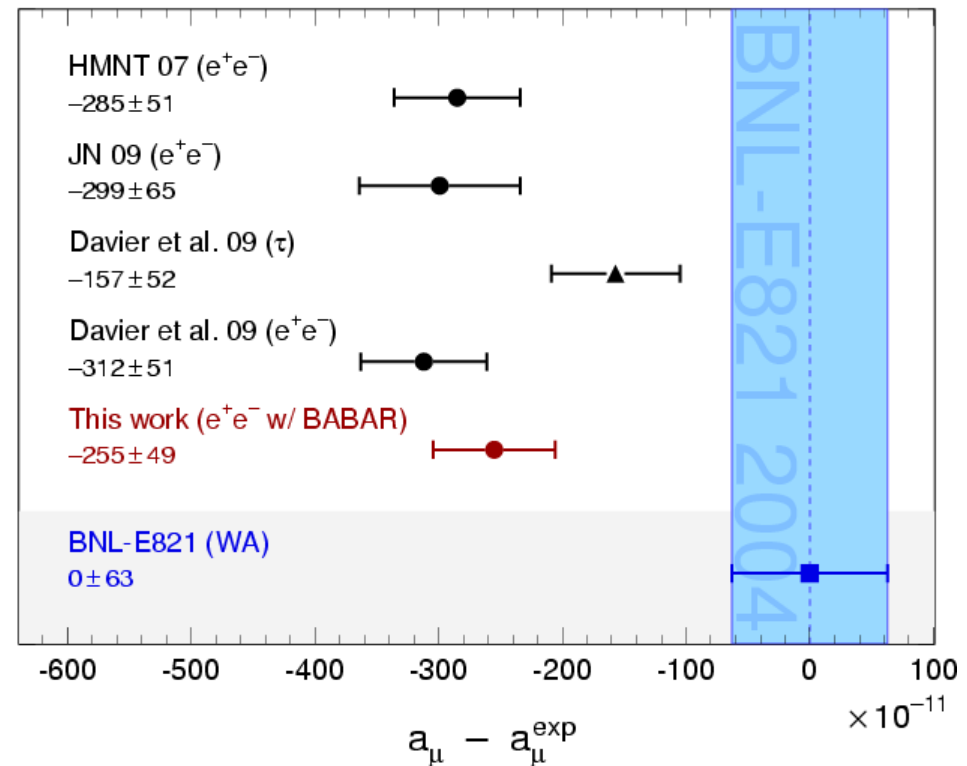
- E-821 updated result

$$11\,659\,208.9 \pm 6.3$$

- deviation (ee)  $25.5 \pm 8.0$   
( $3.2 \sigma$ )

- updated  $\tau$  analysis  
+Belle +revisited IB corrections

- deviation ( $\tau$ )  $15.7 \pm 8.2$   
( $1.9 \sigma$ )



# Discussion

- BaBar  $2\pi$  data complete and the most accurate, but expected precision improvement on the average not reached because of discrepancy with KLOE
- however, previous  $\tau/ee$  disagreement strongly reduced  
 $2.9\sigma$  (2006)  $\rightarrow$   $2.4\sigma$  ( $\tau$  update)  $\rightarrow$   $1.5\sigma$  (including BaBar)
- a range of values for the deviation from the SM can be obtained, depending on the  $2\pi$  data used:

BaBar	$2.4\sigma$
all ee	$3.2\sigma$
all ee – BaBar	$3.7\sigma$
all ee – KLOE	$2.9\sigma$
$\tau$	$1.9\sigma$

- all approaches yield a deviation, but SM test limited by systematic effects not accounted for in the experimental analyses (ee) and/or the corrections to  $\tau$  data
- at the moment some evidence for a deviation ( $2-4\sigma$ ), but not sufficient to establish a contribution from new physics

# Perspectives

- first priority is a clarification of the BaBar/KLOE discrepancy:
  - origin of the 'slope' (was very pronounced with the 2004 KLOE results, reduced now with the 2008 results)
  - normalization difference on  $\rho$  peak (most direct effect on  $a_\mu$ )
  - Novosibirsk results in-between, closer to BaBar
  - slope also seen in KLOE/ $\tau$  comparison; BaBar agrees with  $\tau$
- further checks of the KLOE results are possible: as method is based on MC simulation for ISR and additional ISR/ISR probabilities  $\Rightarrow$  long-awaited test with  $\mu\mu\gamma$  analysis
- contribution from multi-hadronic channels will continue to be updated with more results forthcoming from BaBar, particularly  $2\pi 2\pi^0$
- more ee data expected from VEPP-2000 in Novosibirsk
- experimental error of E-821 direct  $a_\mu$  measurement is a limitation, already now
  - $\Rightarrow$  new proposal submitted to Fermilab to improve accuracy by a factor 4
  - $\Rightarrow$  project at JPARC

# Conclusions

- BaBar analysis of  $\pi\pi$  and  $\mu\mu$  ISR processes completed
- Precision goal has been achieved: 0.5% in  $\rho$  region (0.6-0.9 GeV)
- Absolute  $\mu\mu$  cross section agrees with NLO QED within 1.1%
- $ee \rightarrow \pi\pi(\gamma)$  cross section very insensitive to MC generator
- full range of interest covered from 0.3 to 3 GeV
- Structures observed in pion form factor at large masses
- Comparison with data from earlier experiments
  - fair agreement with CMD-2 and SND, poor with KLOE
  - agreement with  $\tau$  data
- Contribution to  $a_\mu$  from BaBar is  $(514.1 \pm 2.2 \pm 3.1) \times 10^{-10}$  in 0.28-1.8 GeV
- BaBar result has comparable accuracy (0.7%) to combined previous results
- Deviation between BNL measurement and theory prediction reduced using BaBar  $\pi\pi$  data

$$a_\mu [\text{exp}] - a_\mu [\text{SM}] = (19.8 \pm 8.4) \times 10^{-10}$$

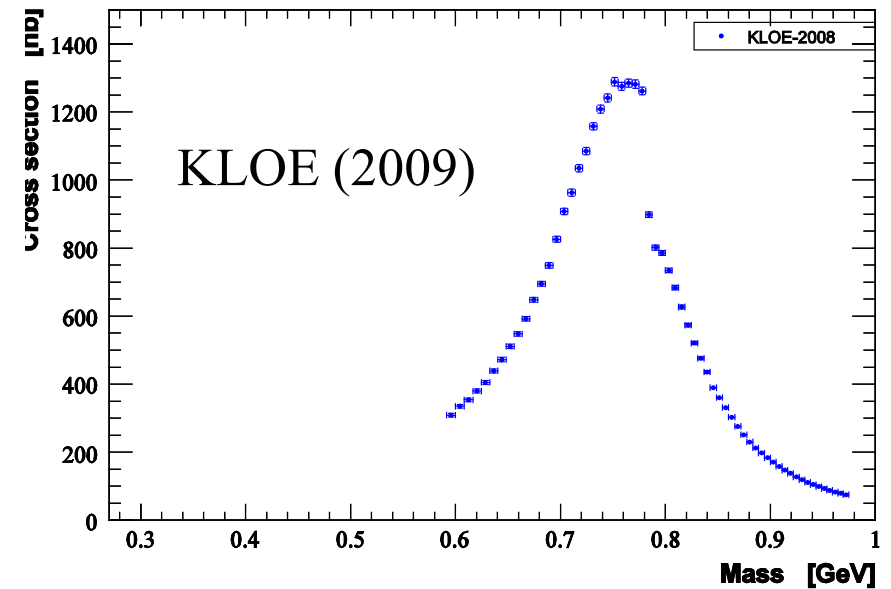
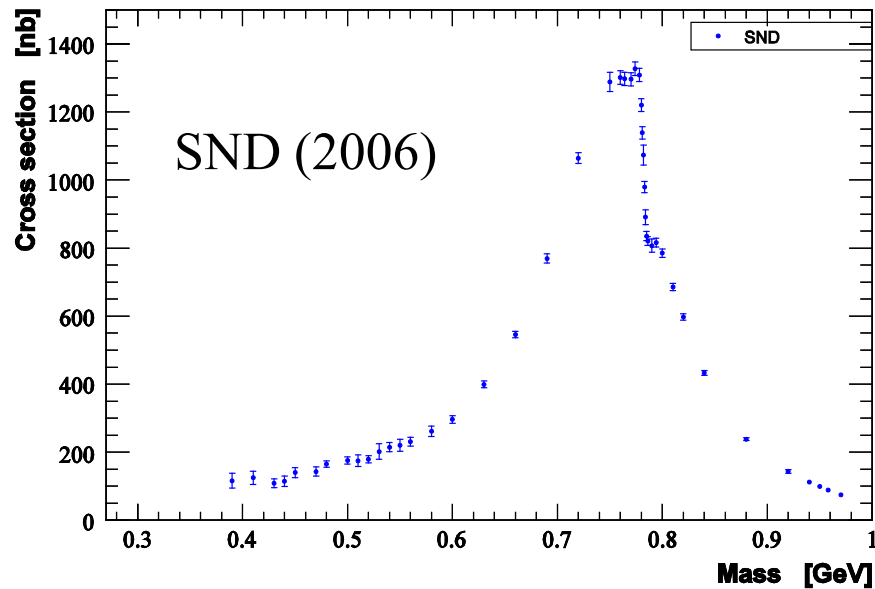
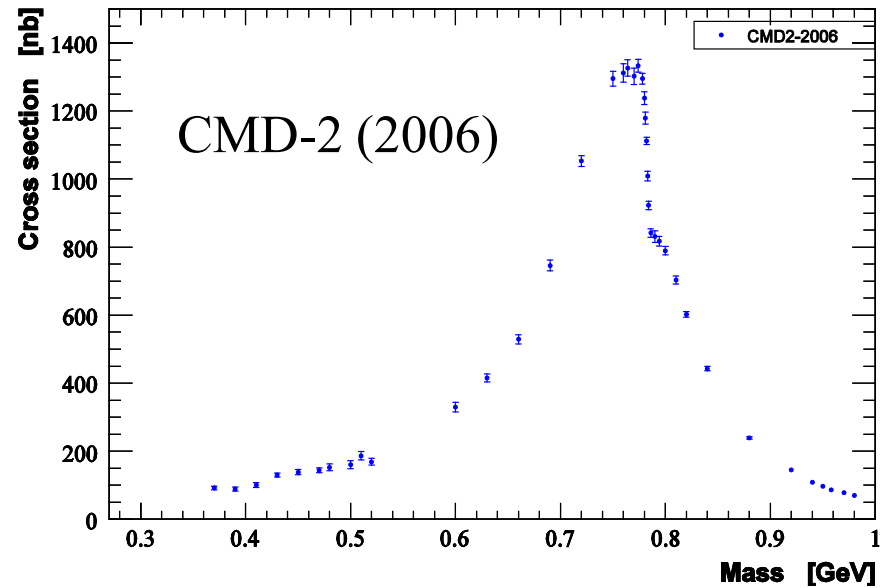
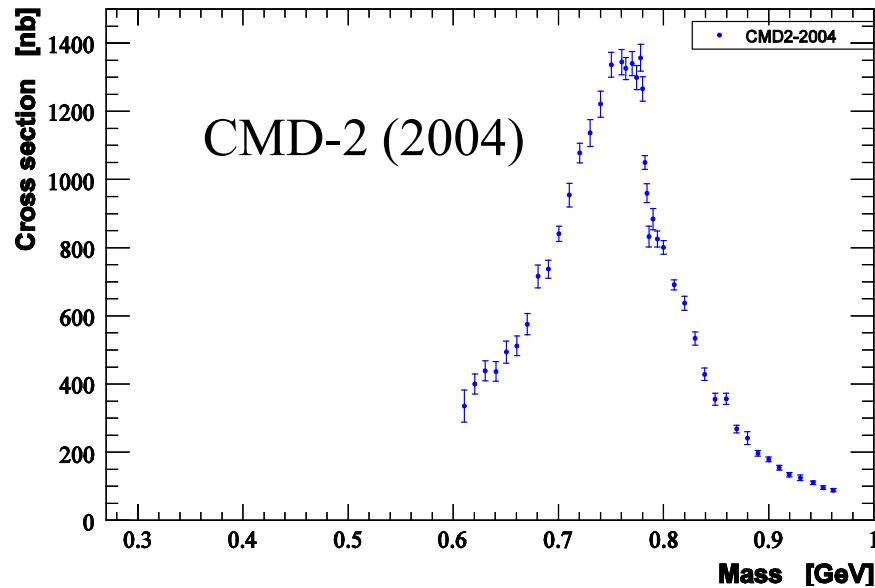
$$25.5 \pm 8.0$$

$2\pi$  from BaBar only

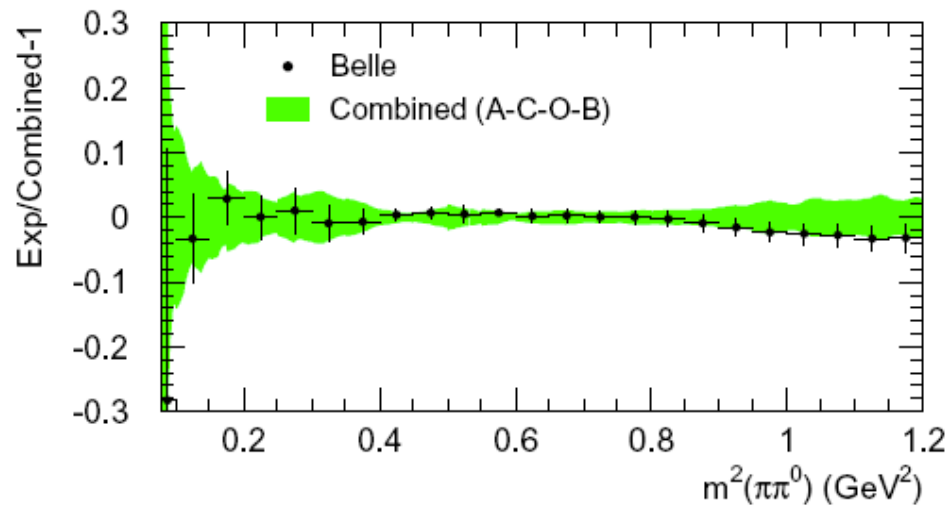
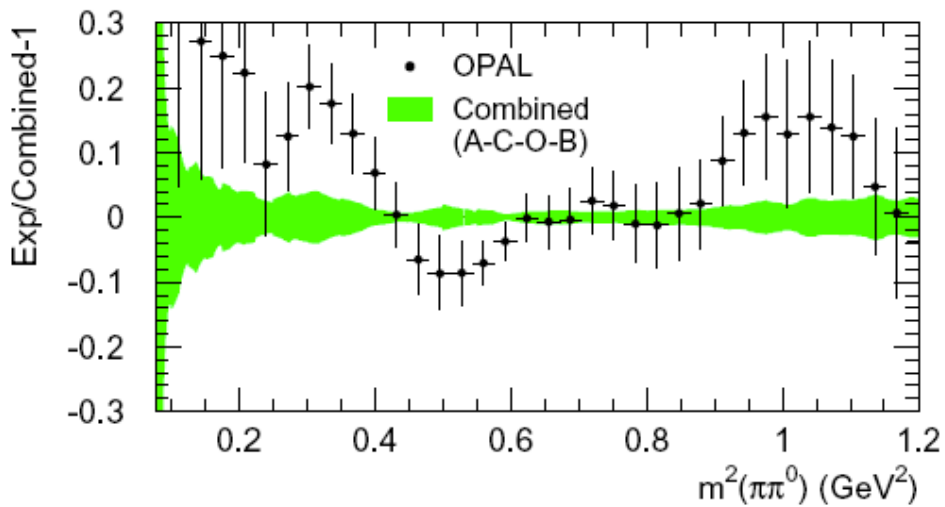
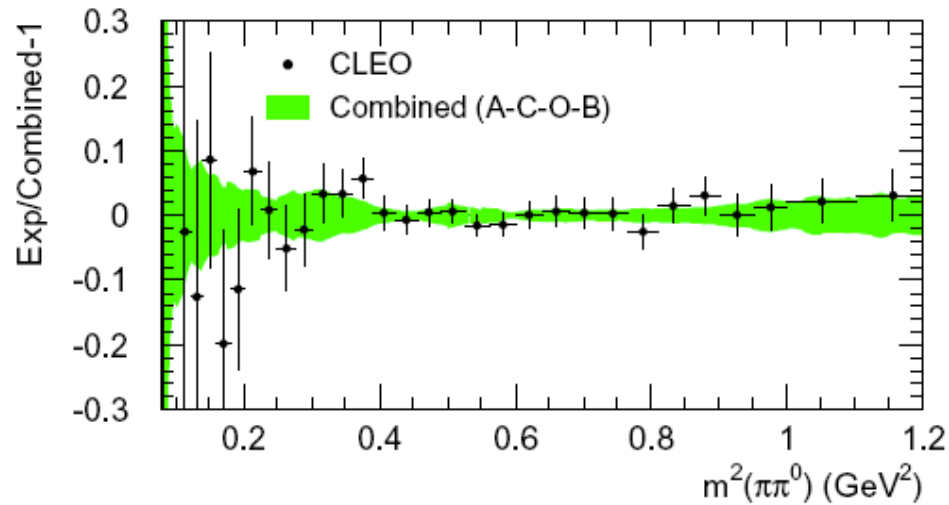
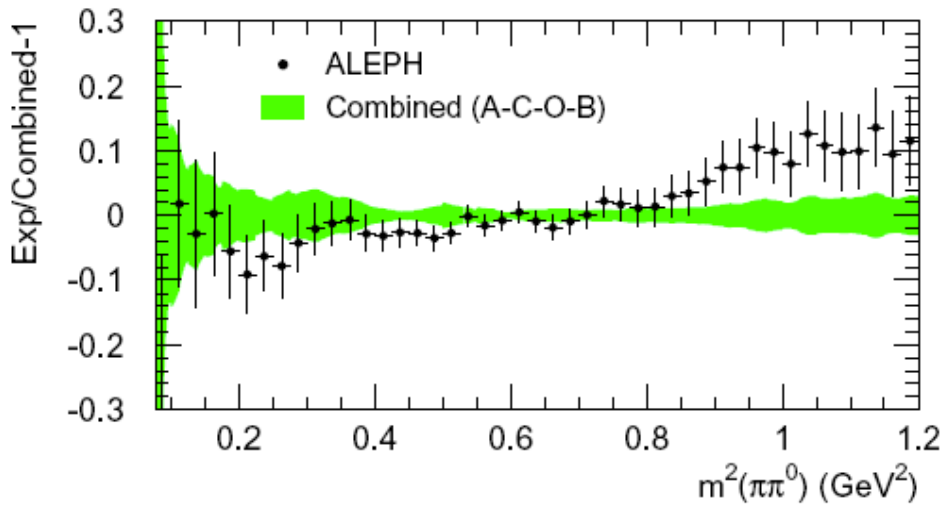
combined ee including BaBar

# Backup Slides

# Data on $e^+e^- \rightarrow \text{hadrons}$



# Revisited Analysis using $\tau$ Data: including Belle



# Revisited Analysis $\tau$ Data: new IB corrections

Source	$\Delta a_\mu^{\text{had,LO}}[\pi\pi, \tau] (10^{-10})$	
	GS model	KS model
$S_{\text{EW}}$	$-12.21 \pm 0.15$	
$G_{\text{EM}}$	$-1.92 \pm 0.90$	
FSR	$+4.67 \pm 0.47$	
$\rho$ - $\omega$ interference	$+2.80 \pm 0.19$	$+2.80 \pm 0.15$
$m_{\pi^\pm} - m_{\pi^0}$ effect on $\sigma$	$-7.88$	
$m_{\pi^\pm} - m_{\pi^0}$ effect on $\Gamma_\rho$	$+4.09$	$+4.02$
$m_{\rho^\pm} - m_{\rho_{\text{bare}}^0}$	$0.20^{+0.27}_{-0.19}$	$0.11^{+0.19}_{-0.11}$
$\pi\pi\gamma$ , electrom. decays	$-5.91 \pm 0.59$	$-6.39 \pm 0.64$
Total	$-16.07 \pm 1.22$	$-16.70 \pm 1.23$
	$-16.07 \pm 1.85$	



# The Measurement

- ISR photon at large angle in EMC
  - 1 (for efficiency) or 2 (for physics) tracks of good quality
  - identification of the charged particles
  - separate  $\pi\pi/\text{KK}/\mu\mu$  event samples
  - kinematic fit (not using ISR photon energy) including 1 additional photon
  - obtain all efficiencies (trigger, filter, tracking, ID, fit) from same data
  - **measure ratio of  $\pi\pi\gamma(\gamma)$  to  $\mu\mu\gamma(\gamma)$  cross sections to cancel**
    - ee luminosity
    - additional ISR
    - vacuum polarization
    - ISR photon efficiency
- } otherwise  $\sim 2\%$  syst error
- correct for  $|\text{FSR}|^2$  contribution in  $\mu\mu\gamma(\gamma)$  (QED,  $<1\%$  below 1 GeV)
  - additional FSR photons measured

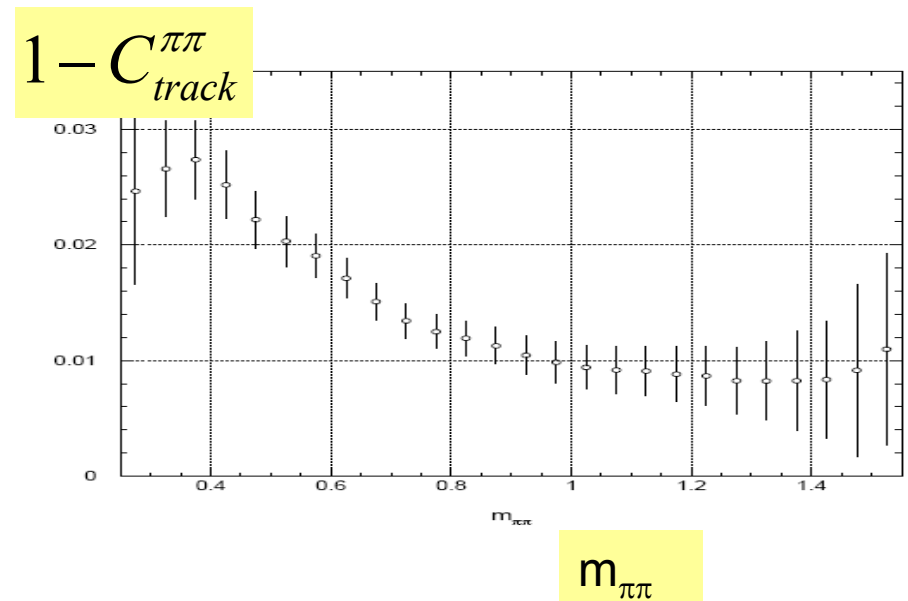
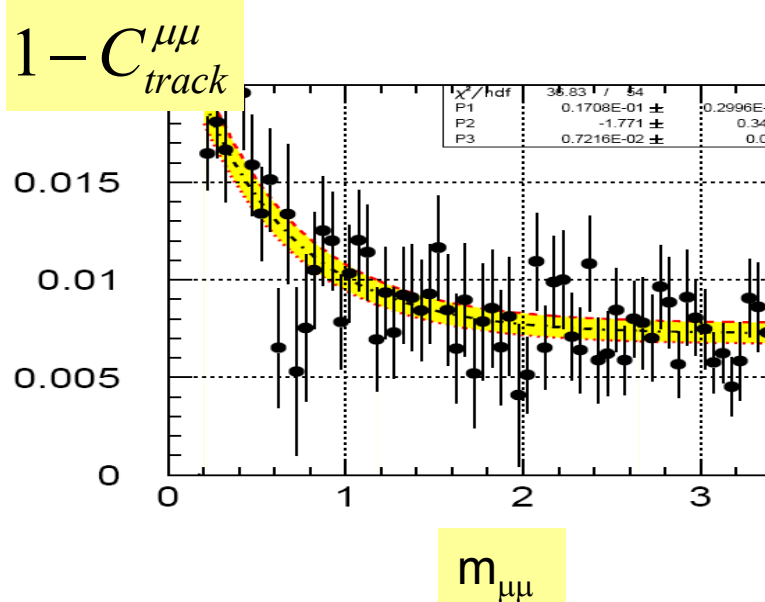
$$R_{\text{exp}}(s') = \frac{\sigma[\pi\pi\gamma(\gamma)](s')}{\sigma[\mu\mu\gamma(\gamma)](s')} = \frac{\sigma_{[\pi\pi(\gamma)]}^0(s')}{(1 + \delta_{\text{FSR}}^{\mu\mu})\sigma_{[\mu\mu(\gamma)]}^0(s')} = \frac{R(s')}{(1 + \delta_{\text{FSR}}^{\mu\mu})(1 + \delta_{\text{add,FSR}}^{\mu\mu})}$$

# Data/MC Tracking Correction to $\pi\pi\gamma, \mu\mu\gamma$ cross sections

- single track efficiency
- correlated loss probability  $f_0$
- probability to produce more than 2 tracks  $f_3$

$$C_{\mu\mu}^{track} = \left( \frac{\varepsilon_{track}^{data}}{\varepsilon_{track}^{MC}} \right)^2 \frac{(1 - f_0 - f_3)^{data}}{(1 - f_0 - f_3)^{MC}}$$

and similarly for  $\pi\pi$



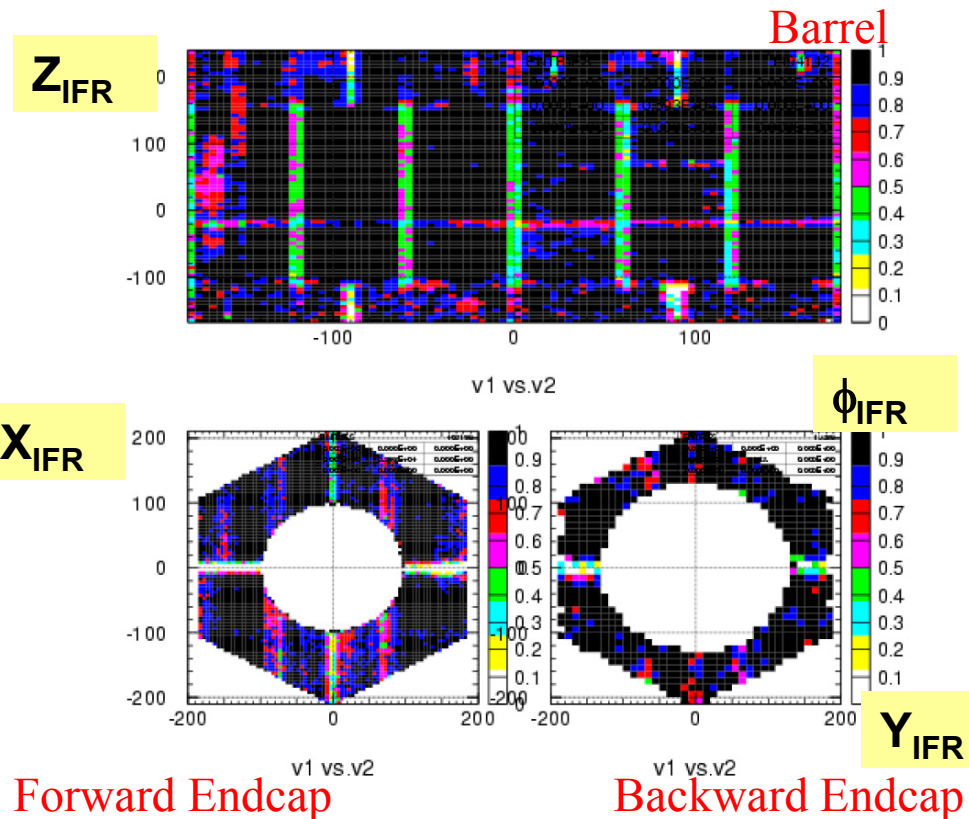
# Particle Identification

- Particle identification required to separate  $XX\gamma$  final processes
- Define 5 ID classes using cuts and PID selectors (complete and orthogonal set)
- Electrons rejected at track definition level ( $E_{\text{cal}}$ ,  $dE/dx$ )
- All ID efficiencies measured

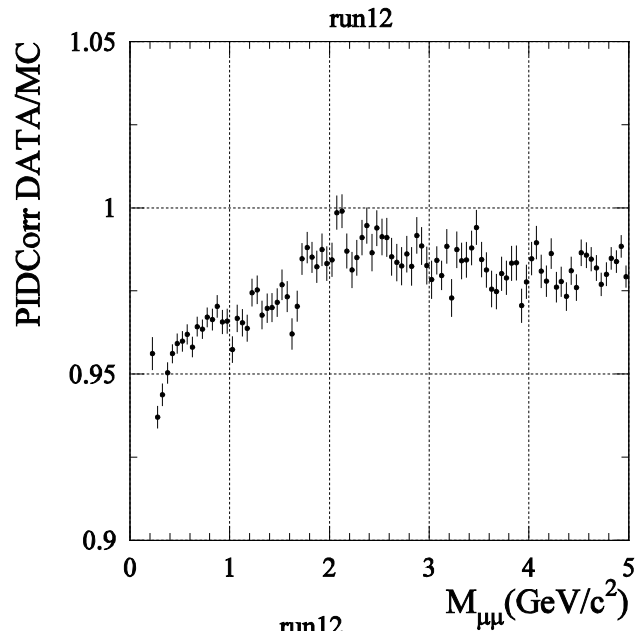
$$\varepsilon_{X \rightarrow I}$$

- a tighter  $\pi$  ID ( $\pi_h$ ) is used for tagging in efficiency measurements and to further reject background in low cross section regions.

- \* isolated muons  $M_{\mu\mu} > 2.5 \text{ GeV}$   
→ efficiency maps ( $p, v_1, v_2$ )  
impurity  $(1.1 \pm 0.1) 10^{-3}$
- \* correlated efficiencies/close tracks  
→ maps ( $dv_1, dv_2$ )

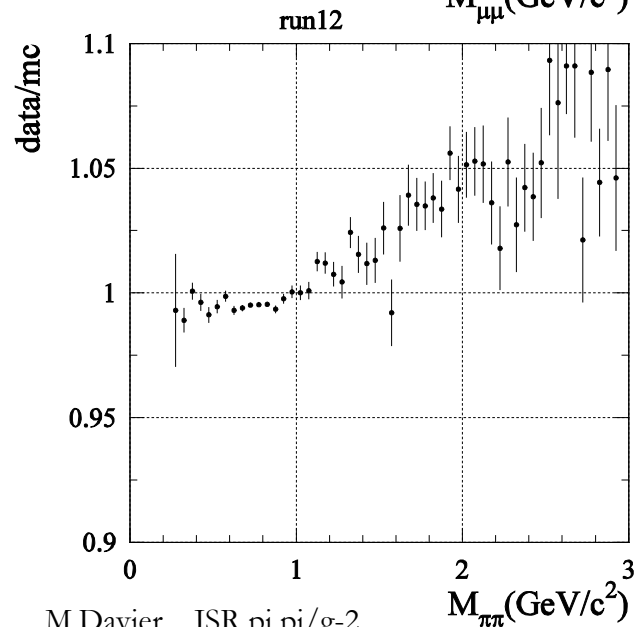
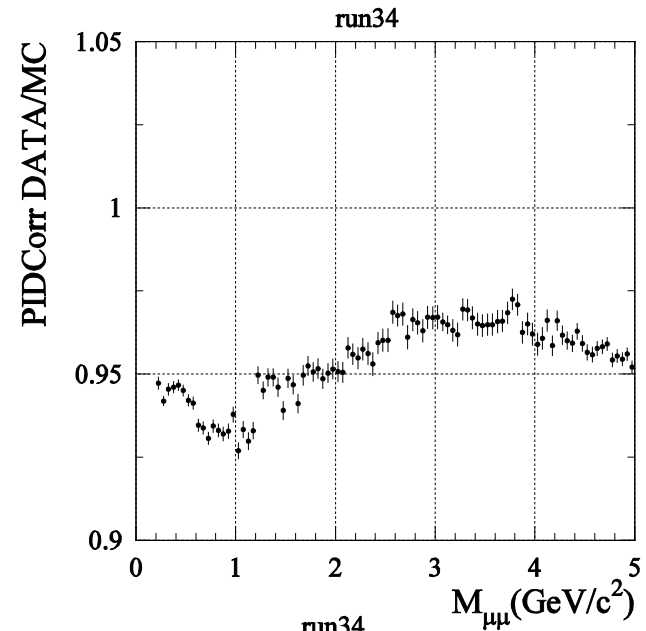


# Data/MC PID corrections to $\mu\mu$ and $\pi\pi$ cross sections

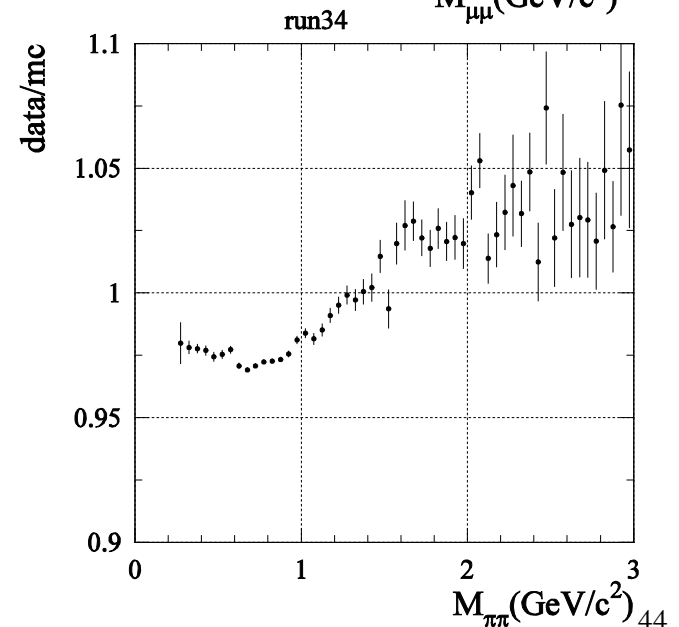


$\mu\mu\gamma$

Two running periods with different IFR performance



$\pi\pi\gamma$

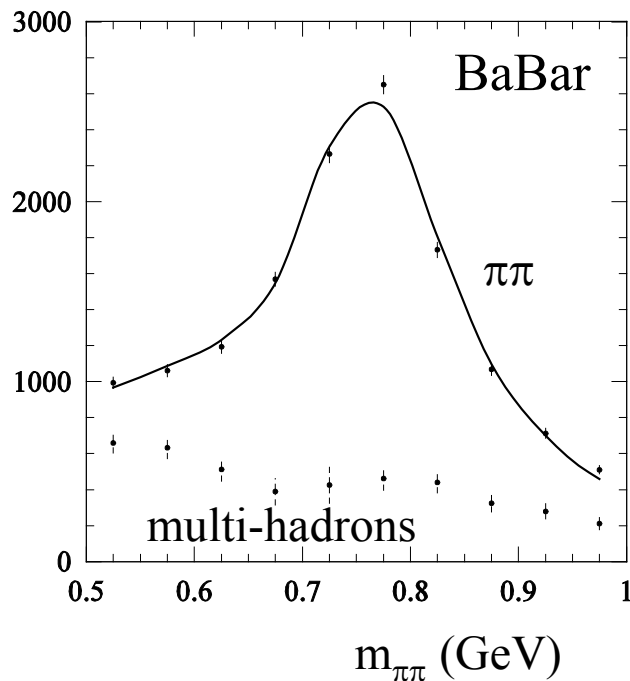


# Backgrounds

- background larger with loose  $\chi^2$  cut used in 0.5-1.0 GeV mass range
- $q\bar{q}$  and multi-hadronic ISR background from MC samples + normalization from data using signals from  $\pi^0 \rightarrow \gamma_{\text{ISR}} \gamma$  ( $q\bar{q}$ ), and  $\omega$  and  $\phi$  ( $\pi\pi\pi^0\gamma$ )
- global test in background-rich region near cut boundary

BG fractions in  $10^{-2}$  at  $m_{\pi\pi}$  values

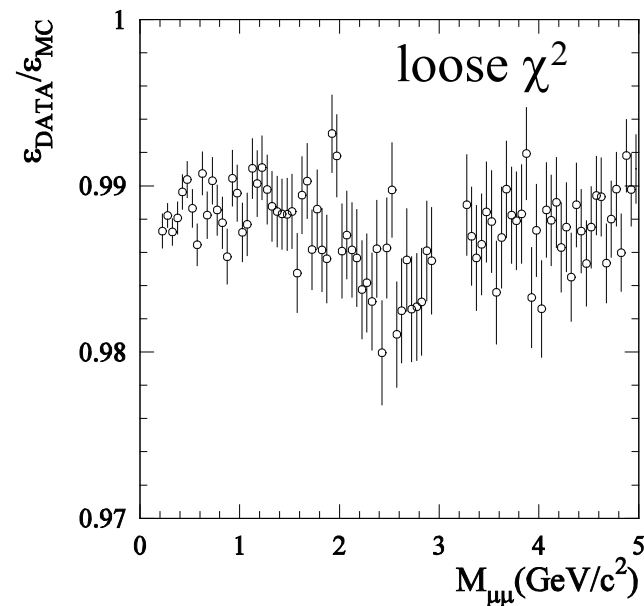
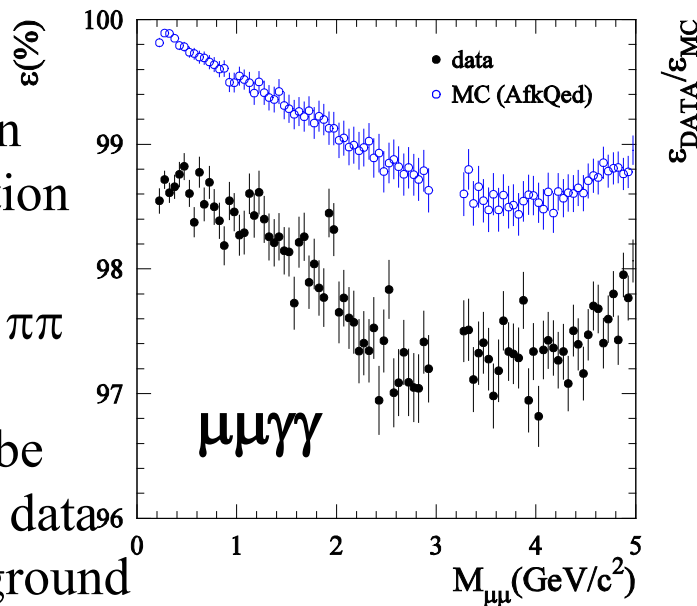
Fitted BG/predicted =  $0.968 \pm 0.037$



process	0.525 GeV	0.775 GeV	0.975 GeV
$\mu\mu$	$3.48 \pm 0.36$	$0.37 \pm 0.23$	$2.71 \pm 0.31$
$KK$	$0.08 \pm 0.01$	$0.01 \pm 0.01$	$0.08 \pm 0.01$
$\gamma 2\pi\pi^0$	$8.04 \pm 0.41$	$0.39 \pm 0.05$	$0.88 \pm 0.19$
$q\bar{q}$	$1.11 \pm 0.17$	$0.26 \pm 0.03$	$1.81 \pm 0.19$
$\gamma 2\pi 2\pi^0$	$1.29 \pm 0.16$	$0.06 \pm 0.01$	$0.46 \pm 0.09$
$\gamma 4\pi$	$0.20 \pm 0.04$	$0.09 \pm 0.01$	$0.24 \pm 0.06$
$\gamma p\bar{p}$	$0.22 \pm 0.02$	$0.04 \pm 0.01$	$0.52 \pm 0.06$
$\gamma \eta 2\pi$	$0.02 \pm 0.01$	$0.03 \pm 0.01$	$0.09 \pm 0.01$
$\gamma K_S K_L$	$0.18 \pm 0.03$	$0.01 \pm 0.01$	$0.10 \pm 0.02$
$\gamma 4\pi 2\pi^0$	$< 0.01$	$< 0.01$	$< 0.01$
$\tau\tau$	$0.17 \pm 0.03$	$0.04 \pm 0.01$	$0.31 \pm 0.05$
$\gamma ee$	$0.63 \pm 0.63$	$0.03 \pm 0.03$	$0.27 \pm 0.27$
total	$15.38 \pm 0.87$	$1.31 \pm 0.24$	$7.37 \pm 0.51$

# $\chi^2$ cut Efficiency Correction

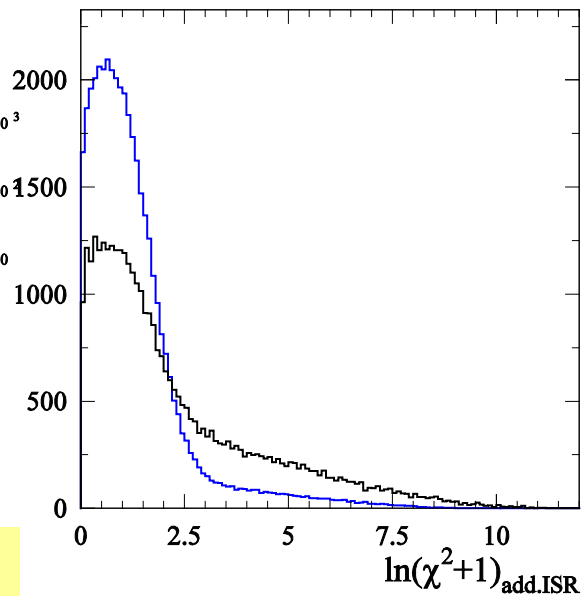
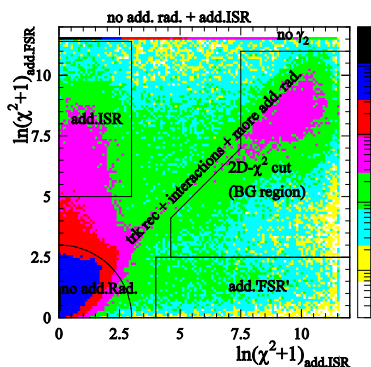
- depends on simulation of ISR (FSR), resolution effects (mostly ISR  $\gamma$  direction) for  $\mu\mu$  and  $\pi\pi$
- $\chi^2$  cut efficiency can be well measured in  $\mu\mu$  data because of low background



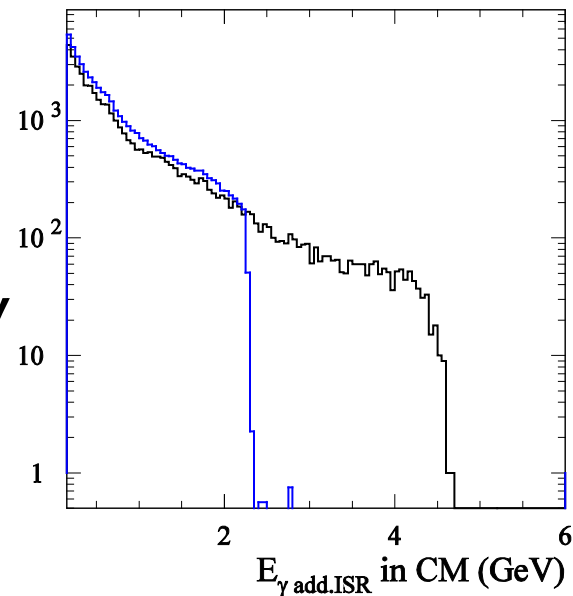
- main correction from lack of angular distribution for additional ISR in AfkQed
- common correction: 1% for loose  $\chi^2$ , 7% for tight  $\chi^2$
- additional loss for  $\pi\pi$  because of interactions studied with sample of interacting events  
much better study now, 2 independent methods

secondary interactions  
 data/MC  $1.51 \pm 0.03$   
 syst error  $0.3 - 0.9 \times 10^{-3}$

# Additional ISR

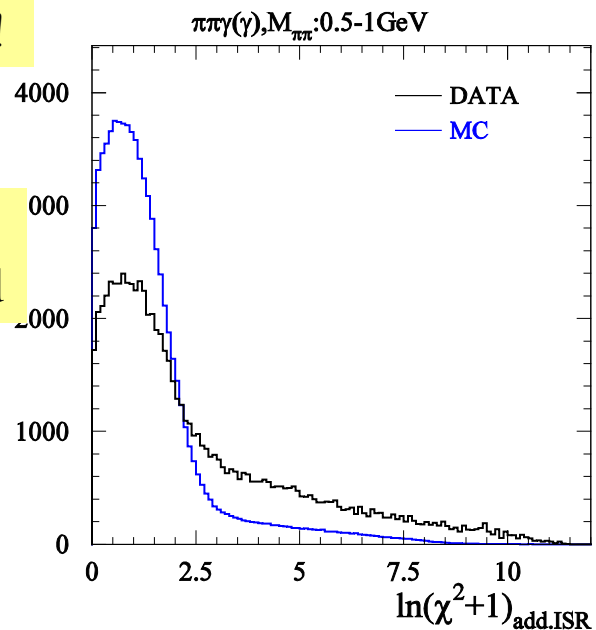


$\mu\mu\gamma\gamma$

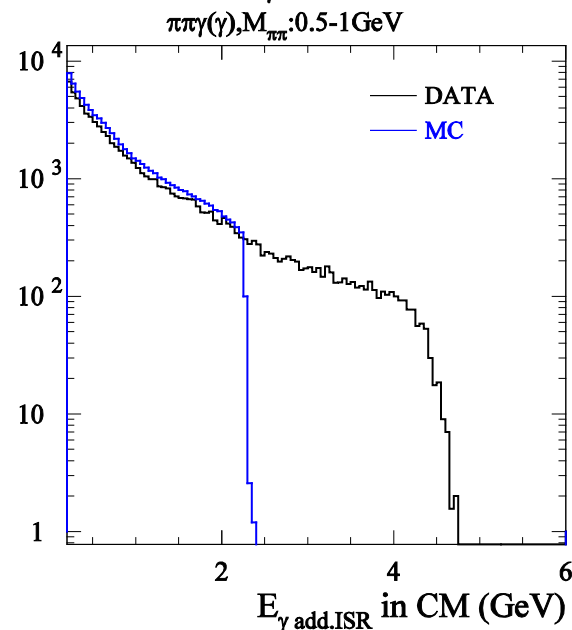


Angular distribution  
of add. ISR /beams!

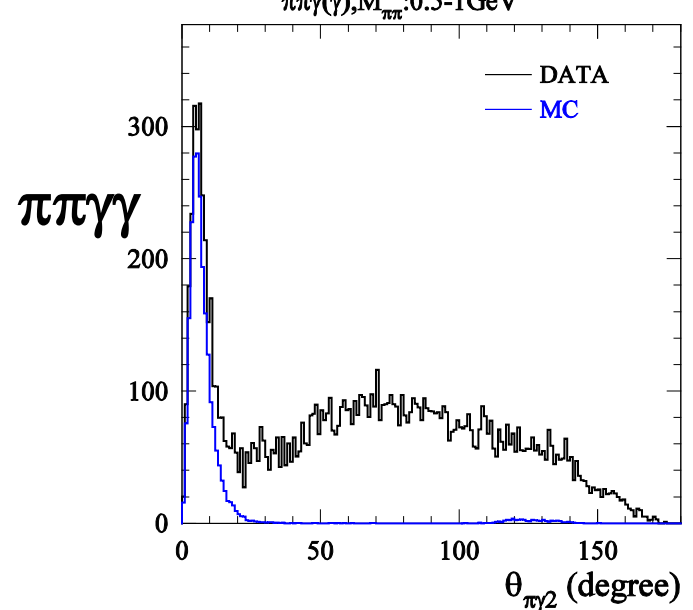
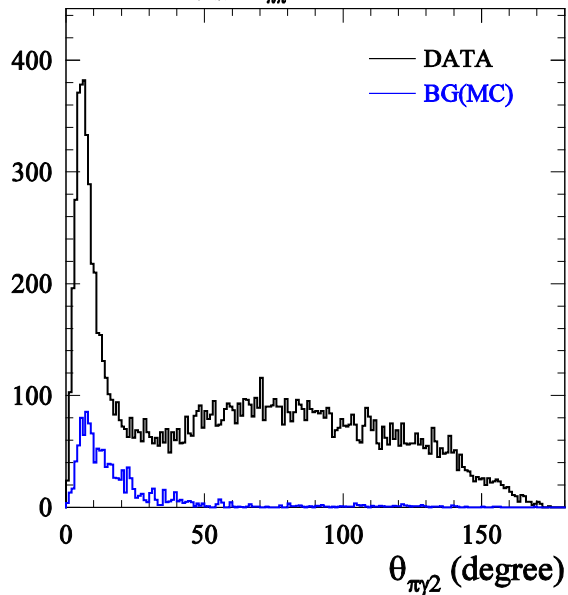
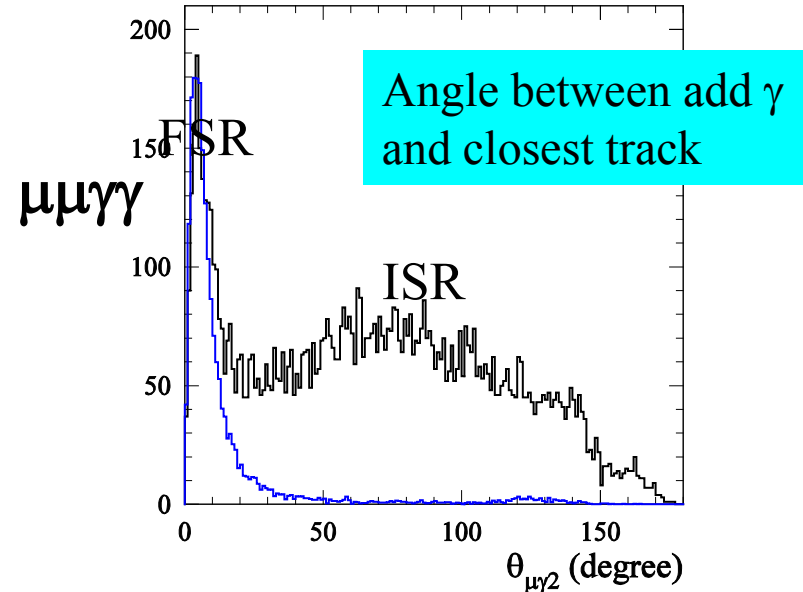
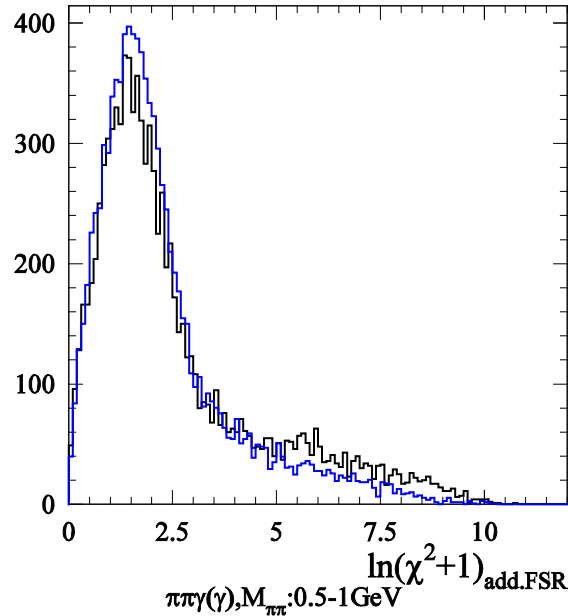
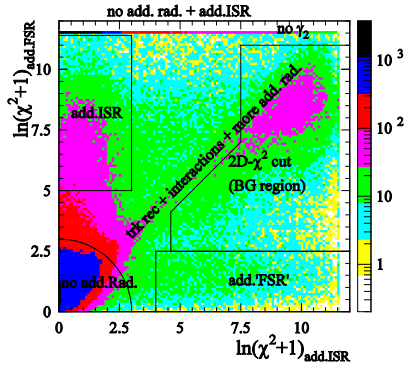
Energy cut-off for  
add. ISR in AfkQed



$\pi\pi\gamma\gamma$



# Additional FSR



Large-angle add.ISR  
in data  $\neq$  AfkQed

Evidence for FSR  
data  $\sim$  AfkQed

data/MC

$\mu\mu$   $0.96 \pm 0.06$

$\pi\pi$   $1.21 \pm 0.05$



# Checking Known Distributions

$\cos\theta^*$  in XX CM  $/\gamma$

$\mu\mu$

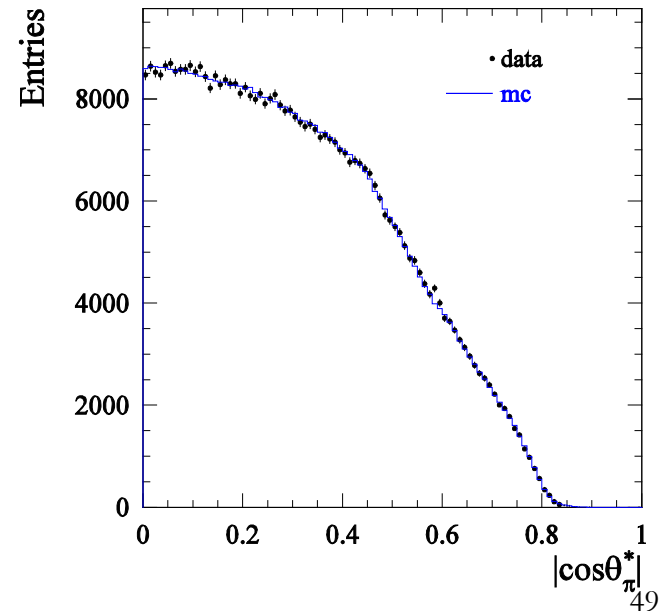
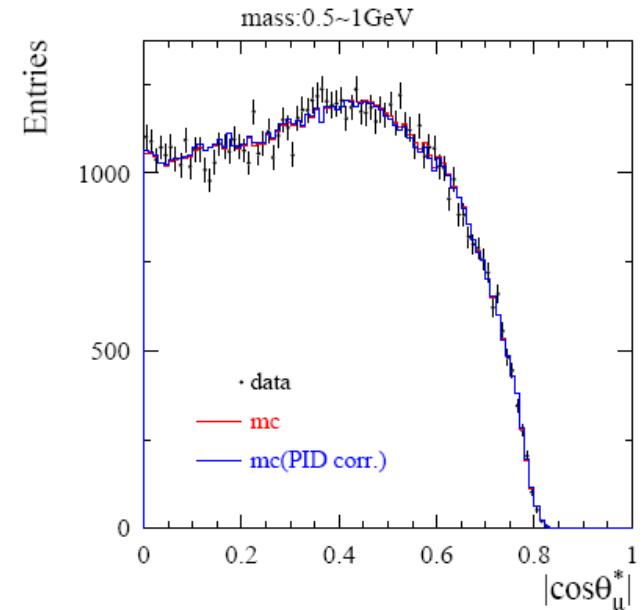
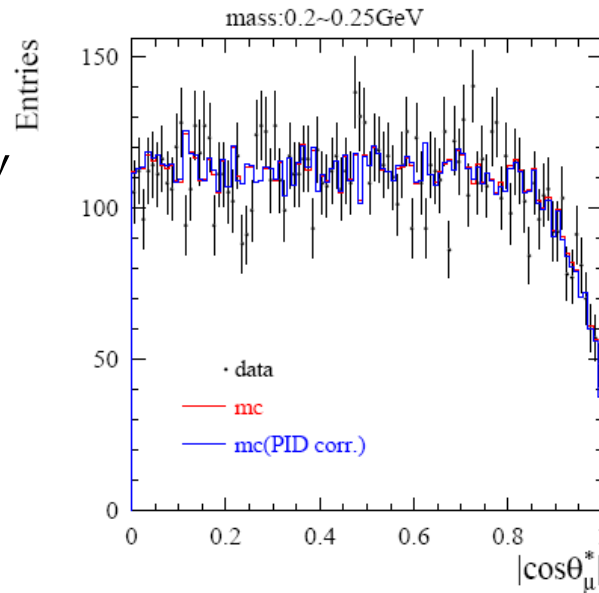
flat at threshold

$1+\cos^2\theta^* \quad \beta_\mu \rightarrow 1$

$\pi\pi$

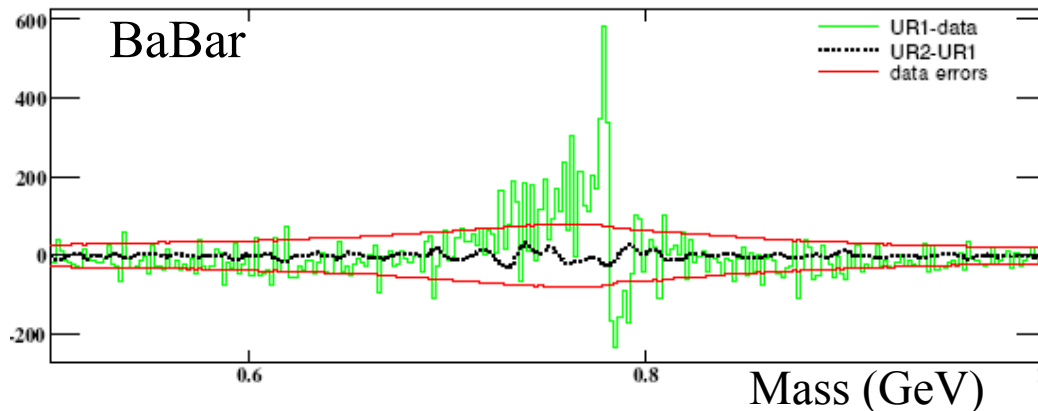
$\sin^2\theta^* \quad \forall \beta_\pi$

$P > 1$  GeV track requirement  $\Rightarrow$  loss at  $\cos\theta^* \sim 1$

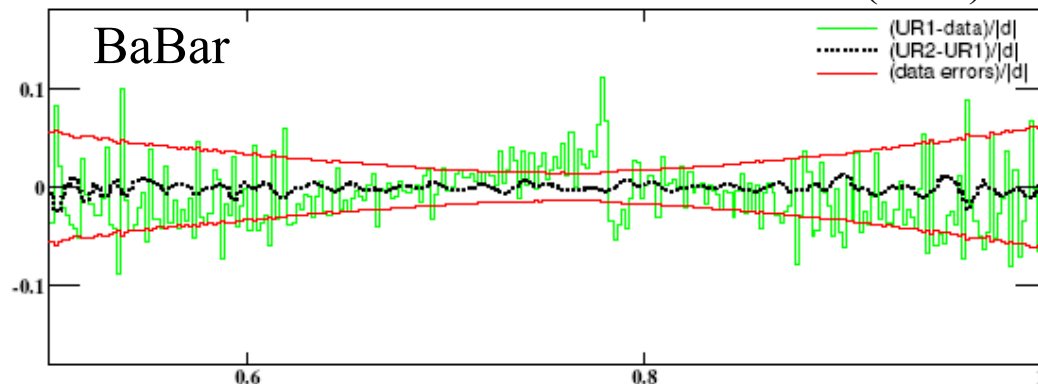


# Unfolding $\pi\pi$ Mass Spectrum

- measured mass spectrum distorted by resolution effects and FSR ( $m_{\pi\pi}$  vs.  $\sqrt{s}$ )
- iterative unfolding method (B. Malaescu arXiv:0907-3791)
- mass-transfer matrix from simulation with corrections from data
- 2 MeV bins in 0.5-1.0 GeV mass range, 10 MeV bins outside
- most salient effect in  $\rho$ - $\omega$  interference region (little effect on  $a_\mu^{\pi\pi}$ )



Absolute difference  
unfolded(1) – raw data  
unfolded(2) – unfolded(1)  
Statistical errors (band)



Relative difference

# Obtaining the $\pi\pi(\gamma)$ cross section

$$\frac{dN_{\pi\pi\gamma(\gamma)}}{d\sqrt{s'}} = \frac{dL_{ISR}^{eff}}{d\sqrt{s'}} \varepsilon_{\pi\pi\gamma(\gamma)}(\sqrt{s'}) \sigma_{\pi\pi(\gamma)}^0(\sqrt{s'})$$

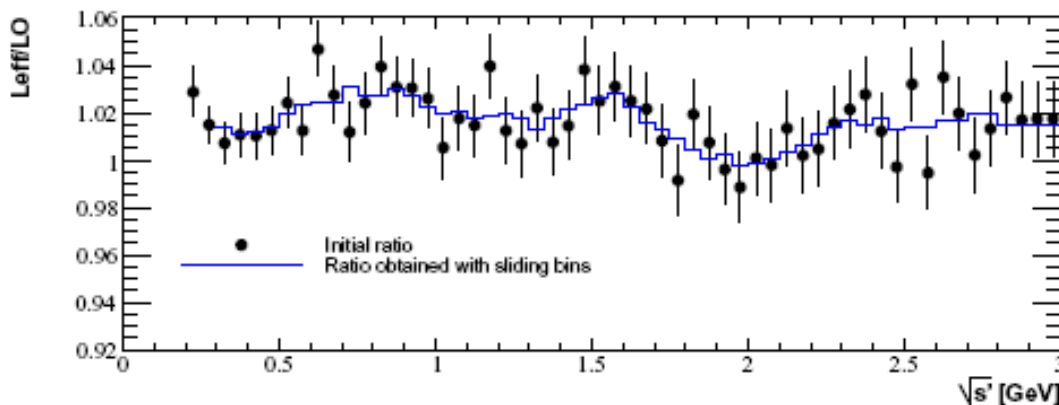
Unfolded spectrum

Acceptance from MC + data/MC corrections

Effective ISR luminosity from  $\mu\mu\gamma(\gamma)$  analysis (similar equation + QED)

Additional ISR almost cancels in the procedure ( $\pi\pi\gamma(\gamma) / \mu\mu\gamma(\gamma)$  ratio)

Correction  $(2.5 \pm 1.0) \cdot 10^{-3} \Rightarrow \pi\pi$  cross section does not rely on accurate description of NLO in the MC generator



ratio  $\mu\mu$  ISR lumi / LO formula should behave smoothly (HVP effects on resonances cancel)

Use measured lumi in 50-MeV bins averaged in sliding 250-MeV bins for smoothing

# Changes since preliminary results at Tau08

- preliminary results Sept. 2008: only 0.5-3 GeV (excess/expect. near threshold)
- problem explored (Oct. 2008- Feb. 2009): trigger/BGFilter, ee background
- $\mu\mu \rightarrow \pi\pi$  re-investigated  $\Rightarrow$  direct measurement achieved using ID probabilities  
 before: model for correlated loss, no precise direct check  
 $\Rightarrow$  significant changes
 

$\mu\mu$ efficiency for ISR lumi	$\Uparrow$	+0.9%
$\mu\mu$ contamination in ' $\pi\pi$ ' sample	$\Downarrow$	
$\Rightarrow \pi\pi$ cross section	$\Downarrow$	
	-1.8%	0.525 GeV
	-1.0%	0.775 GeV
	-1.4%	0.975 GeV
- other changes:
  - MC unfolding mass matrix corrected for data/MC differences (small)
  - ISR lumi now used in 50-MeV sliding bins, instead of global fit
  - cancellation of add ISR in  $\pi\pi/\mu\mu$  ratio studied/corrected
- extensive review

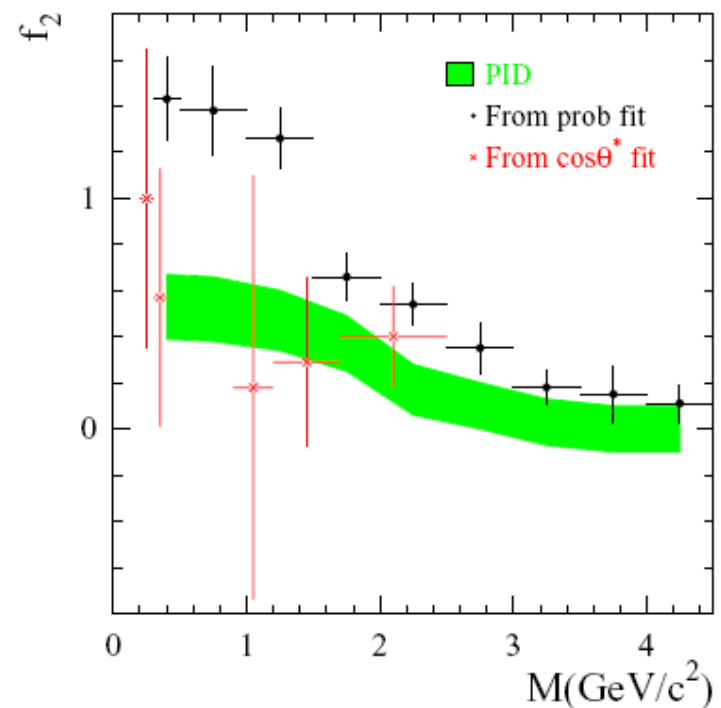
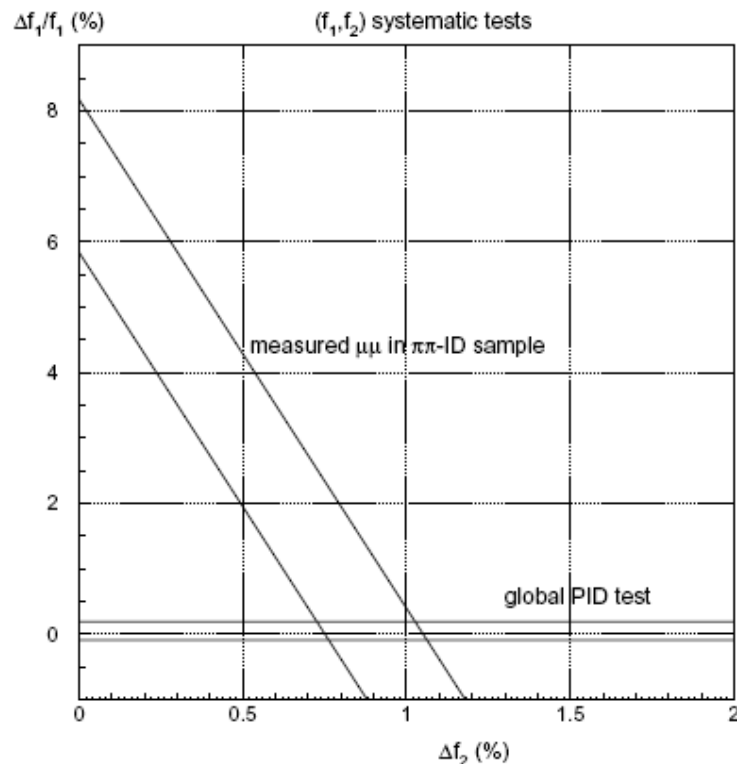
# f<sub>2</sub> Story

$$N_{\mu 1 \mu 2} = N^0 \varepsilon_1 \varepsilon_2 f_1 (1 - f_2)$$

$$N_{\mu 1 \bar{\mu} 2} = N^0 \varepsilon_1 \sqrt{f_1} (1 - \varepsilon_2 \sqrt{f_1}) (1 - f_2)$$

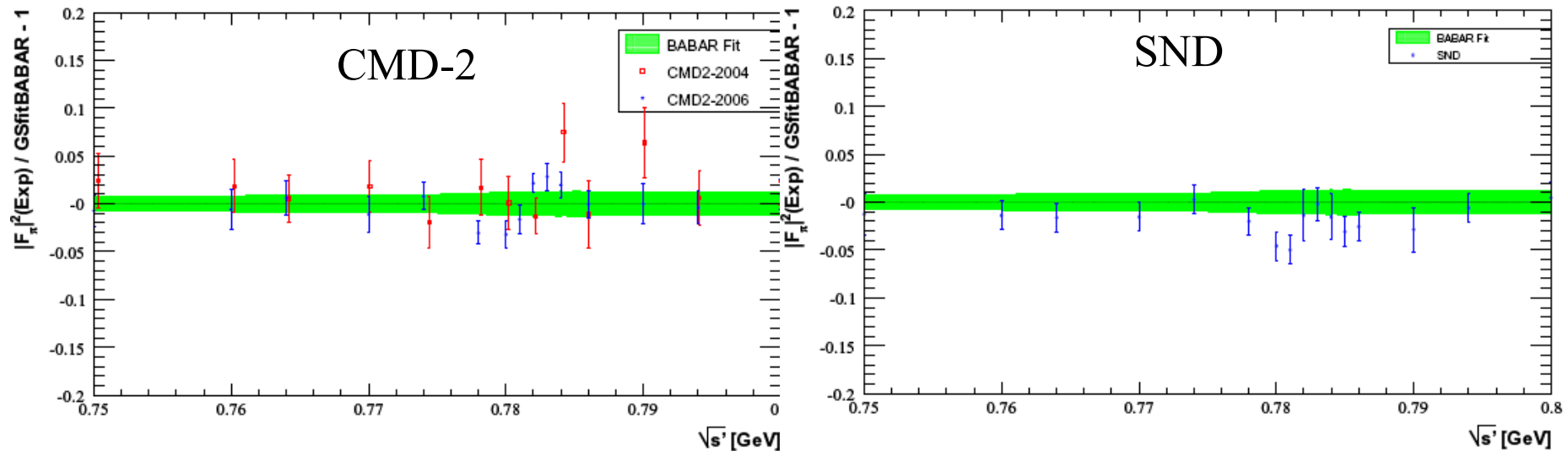
$$N_{\bar{\mu} 1 \mu 2} = N^0 (1 - \varepsilon_1 \sqrt{f_1}) \varepsilon_2 \sqrt{f_1} (1 - f_2)$$

$$N_{\bar{\mu} 1 \bar{\mu} 2} = N^0 [(1 - \varepsilon_1 \sqrt{f_1}) (1 - \varepsilon_2 \sqrt{f_1}) (1 - f_2) + f_2]$$

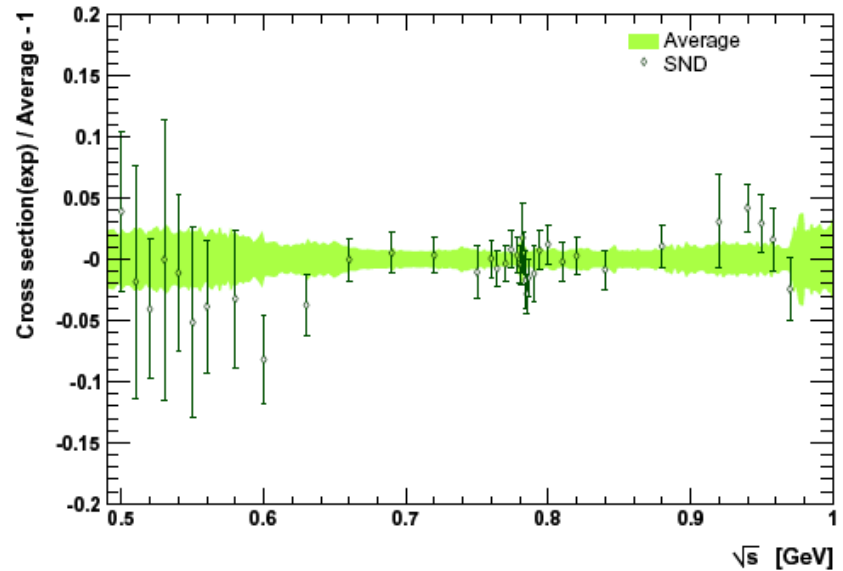
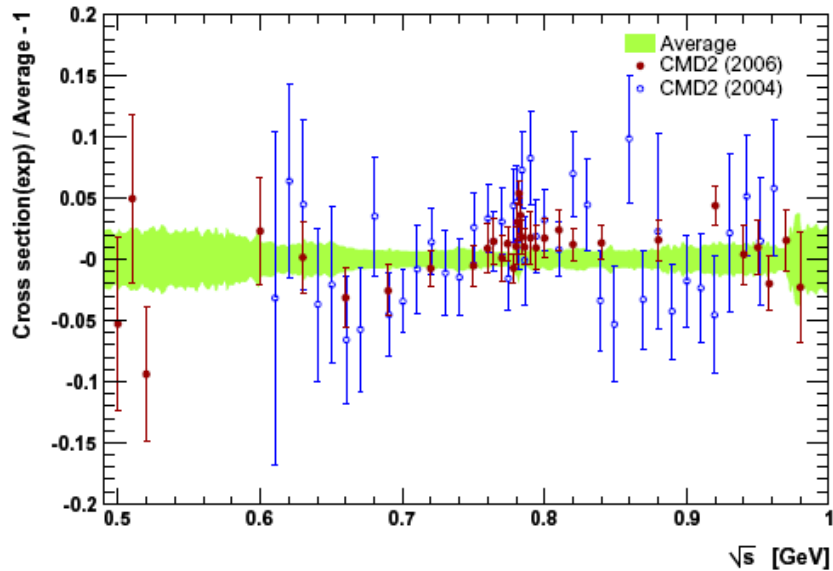
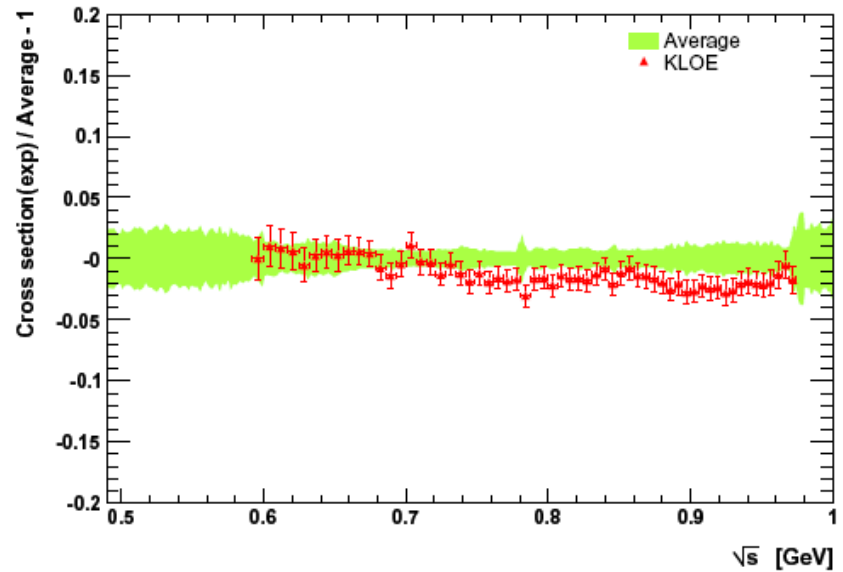
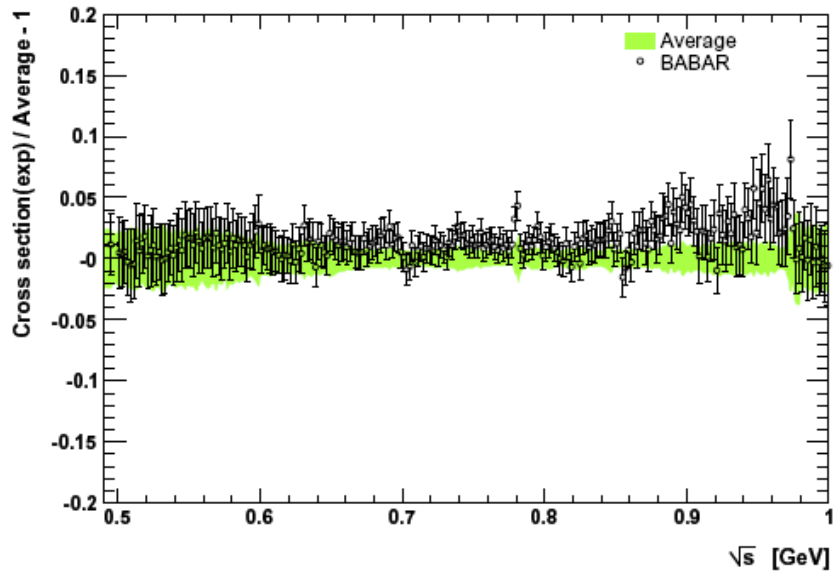


# BaBar vs. other ee data ( $\rho$ - $\omega$ interference region)

- mass calibration of BaBar checked with ISR-produced  $J/\psi \rightarrow \mu\mu$
- expect  $-(0.16 \pm 0.16)$  MeV at  $\rho$  peak
- $\omega$  mass determined through VDM mass fit
$$m_{\omega}^{\text{fit}} - m_{\omega}^{\text{PDG}} = -(0.12 \pm 0.29) \text{ MeV}$$
- Novosibirsk data precisely calibrated using resonant depolarization
- comparison BaBar/CMD-2/SND in  $\rho$ - $\omega$  interference region shows no evidence for a mass shift



# Consistency of Experiments with Average



# Backup Slides

Energy range (GeV)	Experiment	$a_{\mu}^{\text{had,LO}}[\pi\pi] (10^{-10})$
$2m_{\pi^{\pm}} - 0.3$	Combined $e^{+}e^{-}$ (fit)	$0.55 \pm 0.01$
$0.30 - 0.63$	Combined $e^{+}e^{-}$	$132.6 \pm 0.8 \pm 1.0 (1.3_{\text{tot}})$
$0.63 - 0.958$	CMD2 03	$361.8 \pm 2.4 \pm 2.1 (3.2_{\text{tot}})$
	CMD2 06	$360.2 \pm 1.8 \pm 2.8 (3.3_{\text{tot}})$
	SND 06	$360.7 \pm 1.4 \pm 4.7 (4.9_{\text{tot}})$
	KLOE 08	$356.8 \pm 0.4 \pm 3.1 (3.1_{\text{tot}})$
	BABAR 09	$365.2 \pm 1.9 \pm 1.9 (2.7_{\text{tot}})$
	Combined $e^{+}e^{-}$	$360.8 \pm 0.9 \pm 1.8 (2.0_{\text{tot}})$
$0.958 - 1.8$	Combined $e^{+}e^{-}$	$14.4 \pm 0.1 \pm 0.1 (0.2_{\text{tot}})$
Total	Combined $e^{+}e^{-}$	$508.4 \pm 1.3 \pm 2.6 (2.9_{\text{tot}})$
Total	Combined $\tau$ [1]	$515.2 \pm 2.0_{\text{exp}} \pm 2.2_{\text{B}} \pm 1.6_{\text{IB}} (3.4_{\text{tot}})$



# Backup Slides

